Konrad-Zuse-Zentrum
für Informationstechnik Berlin

Takustraße 7
D-14195 Berlin-Dahlem
Germany

CORINNA KLAPPROTH, ANTON SCHIELA, AND
PETER DEUFLHARD

Adaptive Timestep Control for the Contact–Stabilized Newmark Method[1]

[1]Supported by the DFG Research Center MATHEON, "Mathematics for key technologies: Modelling, simulation, and optimization of real-world processes", Berlin

ZIB-Report 10-09 (June 2010)

Adaptive Timestep Control for the Contact–Stabilized Newmark Method†

Corinna Klapproth, Anton Schiela, and Peter Deuflhard

June 25, 2010

Abstract

The aim of this paper is to devise an adaptive timestep control in the contact–stabilized Newmark method (ContacX) for dynamical contact problems between two viscoelastic bodies in the framework of Signorini's condition. In order to construct a comparative scheme of higher order accuracy, we extend extrapolation techniques. This approach demands a subtle theoretical investigation of an asymptotic error expansion of the contact–stabilized Newmark scheme. On the basis of theoretical insight and numerical observations, we suggest an error estimator and a timestep selection which also cover the presence of contact. Finally, we give a numerical example.

AMS MSC 2010: 35L86, 74M15, 65K15, 65L06

Keywords: dynamical contact problems, contact–stabilized Newmark method, extrapolation methods, adaptivity, timestep control

1 Introduction

Dynamical contact problems arise in different applications such as biomechanics. In classical approaches, they are modelled via Signorini's contact conditions which are based on the non-penetration of mass. Both in analytical models and in numerical schemes, the resulting nonsmooth and nonlinear variational inequalities give rise to fundamental mathematical difficulties.

Concerning the time discretization of dynamical contact problems, the Newmark method is one of the most popular numerical integrators. As it is well-known, the classical scheme may lead to artificial numerical oscillations at dynamical contact boundaries, and even an undesirable energy blow-up during time integration may occur [6, 19]. In [13], Kane, Repetto, Ortiz, and Marsden introduced an improved

†Supported by the DFG Research Center Matheon, "Mathematics for key technologies: Modelling, simulation, and optimization of real-world processes", Berlin

variant of Newmark's method which is energy dissipative at contact, but still unable to avoid the oscillations at contact boundaries. For this reason, Deuflhard, Krause, and Ertel suggested a *contact–stabilized* Newmark method [6, 19] which avoids the unphysical oscillations and is still energy dissipative at contact. This is the time integration scheme of interest in the present paper.

In view of challenging real life problems (e.g., the motion of a human knee, see [19]), an adaptive control of timestep is of crucial importance in order to increase the efficiency of the contact–stabilized Newmark method (called CSN further on). A mesh of equidistant timesteps can not be expected to be adequate for reaching a given accuracy of the approximation of a reasonable computational effort.

The construction of an adaptive timestep control requires a realistic estimation of the consistency error (cf., e.g., the textbook [5]). As a necessary preparatory step, we studied the stability of dynamical contact problems under perturbation of the initial data [16]. For viscoelastic materials, we found a characterization of a class of problems for which a perturbation result can be expected even in the presence of contact. This gave us the idea about a specific norm in function space which has been exploited for the estimation of the consistency error of Newmark methods. In the unconstrained situation, the symmetric Newmark scheme is equivalent to the Störmer-Verlet scheme which is well–known to be second order consistent (see, e.g., [12]). In the constrained situation, we have proven an estimate for the consistency error of the classical Newmark method, the modified Newmark method by Kane et al., and the contact–stabilized Newmark method under the assumption of bounded total variation of the solution [17].

The paper is organized as follows. We will start with a short exposition of the dynamical Signorini contact problem and the contact–stabilized Newmark method in Section 2. Further, we will sum up known consistency and sensitivity results for the scheme. In Section 3, we will analyze the existence of an asymptotic error expansion of the discretization error theoretically as well as numerically. These results are the basis for the application of modified extrapolation methods in order to construct a comparative scheme of higher order. Finally, in Section 4, we will suggest a problem-adapted error estimator and a suitable timestep selection (called ContacX). We will conclude the paper by a numerical example in Section 5.

2 Notation and Background

In order to fix notation, we write down the classical contact problem formulation for linearly viscoelastic materials via Signorini's contact conditions. Afterwards, we present the corresponding contact–stabilized Newmark method, and we review existing sensitivity and consistency results for the scheme.

2.1 Problem formulation

Our model for dynamical contact between two bodies is based on linearized Signorini's contact conditions. In view of existing perturbation and consistency results, see [16] and [17], we consider linear viscoelastic bodies fulfilling the Kelvin-Voigt constitutive law. For the convenience of the reader, here we merely collect the notation used therein.

Notation. Let the two bodies be identified with the union of two domains which are understood to be bounded subsets in $\mathbb{R}^d$ with $d = 2, 3$. Each of the boundaries are assumed to be Lipschitz and decomposed into three disjoint parts: Γ_D, the Dirichlet boundary, Γ_N, the Neumann boundary, and Γ_C, the possible contact boundary. The actual contact boundary is not known in advance, but is assumed to be contained in a compact strict subset of Γ_C. The Dirichlet boundary conditions give rise to $\mathbf{H}^1_D := \{\mathbf{v} \,|\, \mathbf{v} \in \mathbf{H}^1,\, \mathbf{v}|_{\Gamma_D} = 0\}$.

Tensor and vector quantities are written in bold characters, e.g., $\mathbf{v}$. Time derivatives are indicated by dots ($\dot{}$). For the sake of clear arrangement, we use the abbreviation $\bar{\mathbf{v}} = (\mathbf{v}, \dot{\mathbf{v}})$ for a function and its first time derivative.

For given Banach space $\mathbf{V}$ and time interval $t_0 < T < \infty$, let $C([t_0, T], \mathbf{V})$ be the continuous functions $\mathbf{v} : [t_0, T] \to \mathbf{V}$. The space $\mathbf{L}^2(t_0, T; \mathbf{V})$ consists of all measurable functions $\mathbf{v} : (t_0, T) \to \mathbf{V}$ for which $\|\mathbf{v}\|^2_{\mathbf{L}^2(t_0,T;\mathbf{V})} := \int_{t_0}^T \|\mathbf{v}(t)\|^2_{\mathbf{V}}\, dt < \infty$ holds. We identify $\mathbf{L}^2$ with its dual space and obtain the evolution triple $\mathbf{H}^1 \subset \mathbf{L}^2 \subset (\mathbf{H}^1)^*$ where we denote the dual space to $\mathbf{H}^1$ by $(\mathbf{H}^1)^*$. With reference to this evolution triple, the Sobolev space $\mathbf{W}^{1,2}(t_0, T; \mathbf{H}^1, \mathbf{L}^2)$ means the set of all functions $\mathbf{v} \in \mathbf{L}^2(t_0, T; \mathbf{H}^1)$ that have generalized derivatives $\dot{\mathbf{v}} \in \mathbf{L}^2(t_0, T; (\mathbf{H}^1)^*)$, see, e.g., [24].

We will need the (total) variation $\mathrm{TV}(\mathbf{v}, [t_0, T], \mathbf{V})$ of a function $\mathbf{v} : [t_0, T] \to \mathbf{V}$. The set of all functions from $[t_0, T]$ into $\mathbf{V}$ that have bounded variation is denoted by $\mathrm{BV}([t_0, T], \mathbf{V})$, compare, e.g., [22].

Non-penetration condition. At the contact interface Γ_C, the two bodies may come into contact but must not penetrate each other. We assume a bijective mapping $\phi : \Gamma_C^S \longrightarrow \Gamma_C^M$ between the two possible contact surfaces to be given. Following [8], we define linearized non-penetration with respect to ϕ by

$$[\mathbf{u} \cdot \boldsymbol{\nu}]_\phi(x, t) = \mathbf{u}^S(x, t) \cdot \boldsymbol{\nu}_\phi(x) - \mathbf{u}^M(\phi(x), t) \cdot \boldsymbol{\nu}_\phi(x) \le g(x)\,, \quad x \in \Gamma_C^S\,.$$

This condition is given with respect to the initial gap

$$\Gamma_C^S \ni x \mapsto g(x) = |x - \phi(x)| \in \mathbb{R}$$

between the two bodies in the reference configuration, and we have set

$$\boldsymbol{\nu}_\phi = \begin{cases} \dfrac{\phi(x) - x}{|\phi(x) - x|}\,, & \text{if} \quad x \neq \phi(x)\,, \\ \boldsymbol{\mu}^S(x) = -\boldsymbol{\mu}^M(x)\,, & \text{if} \quad x = \phi(x)\,. \end{cases}$$

Variational problem formulation. For the weak formulation of the dynamical contact problem, the convex set of all admissible displacements is denoted by

$$\mathcal{K} = \{\mathbf{v} \in \mathbf{H}^1_D \,|\, [\mathbf{v} \cdot \boldsymbol{\nu}]_\phi \leq g\} . \tag{1}$$

The materials under consideration are assumed to be linearly viscoelastic, i.e. the stresses satisfy the Kelvin-Voigt constitutive relation. Both elasticity and viscoelasticity tensors should be sufficiently smooth, symmetric, and uniformly positive definite.

The external forces are represented by a linear functional f_{ext} on $\mathbf{H}^1_D$ which accounts for the volume forces and the tractions on the Neumann boundary. The internal forces can be written as a bilinear form a in $\mathbf{H}^1$ for the linearly elastic part, respectively b for the viscous part. Both bilinear forms are bounded in $\mathbf{H}^1$ and give rise to seminorms $\|\cdot\|_a^2 = a(\cdot,\cdot)$ and $\|\cdot\|_b^2 = b(\cdot,\cdot)$. The sum of internal elastic and external forces can be represented by

$$\langle \mathbf{F}(\mathbf{w}), \mathbf{v}\rangle_{(\mathbf{H}^1)^* \times \mathbf{H}^1} = a(\mathbf{w},\mathbf{v}) - f_{\text{ext}}(\mathbf{v}) , \qquad \mathbf{v}, \mathbf{w} \in \mathbf{H}^1 ,$$

and the viscoelastic forces can be written as

$$\langle \mathbf{G}(\mathbf{w}), \mathbf{v}\rangle_{(\mathbf{H}^1)^* \times \mathbf{H}^1} = b(\mathbf{w},\mathbf{v}) , \qquad \mathbf{v}, \mathbf{w} \in \mathbf{H}^1 .$$

Via integration by parts and exploiting the boundary conditions, see [7] and [14], the contact problem in the weak formulation can be written as a variational inequality: For almost every $t \in [0,T]$, find $\mathbf{u} \in \mathcal{K}$ with $\mathbf{u}(\cdot,t) \in C([0,T],\mathbf{H}^1)$ and $\dot{\mathbf{u}} \in \mathbf{W}^{1,2}(0,T;\mathbf{H}^1,\mathbf{L}^2)$ such that for all $\mathbf{v} \in \mathcal{K}$

$$\langle \ddot{\mathbf{u}}, \mathbf{v}-\mathbf{u}\rangle_{(\mathbf{H}^1)^* \times \mathbf{H}^1} + \langle \mathbf{F}(\mathbf{u}), \mathbf{v}-\mathbf{u}\rangle_{(\mathbf{H}^1)^* \times \mathbf{H}^1} + \langle \mathbf{G}(\dot{\mathbf{u}}), \mathbf{v}-\mathbf{u}\rangle_{(\mathbf{H}^1)^* \times \mathbf{H}^1} \geq 0 \tag{2}$$

and

$$\mathbf{u}(0) = \mathbf{u}_0 , \quad \dot{\mathbf{u}}(0) = \dot{\mathbf{u}}_0 . \tag{3}$$

Incorporating the constraints $\mathbf{v}(t) \in \mathcal{K}$ for almost every $t \in [0,T]$ by the characteristic functional $I_{\mathcal{K}}(\mathbf{v})$, the variational inequality (2) can equivalently be formulated as the variational inclusion

$$0 \in \ddot{\mathbf{u}} + \mathbf{F}(\mathbf{u}) + \mathbf{G}(\dot{\mathbf{u}}) + \partial I_{\mathcal{K}}(\mathbf{u})$$

utilizing the subdifferential $\partial I_{\mathcal{K}}$ of $I_{\mathcal{K}}$ (see, e.g., [9]). For a given solution $\mathbf{u}$ of this variational inequality and for almost every $t \in [0,T]$, we define the contact forces $\mathbf{F}_{\text{con}}(\mathbf{u}) \in (\mathbf{H}^1)^*$ by

$$\langle \mathbf{F}_{\text{con}}(\mathbf{u}), \mathbf{v}\rangle_{(\mathbf{H}^1)^* \times \mathbf{H}^1} = \langle \ddot{\mathbf{u}} + \mathbf{F}(\mathbf{u}) + \mathbf{G}(\dot{\mathbf{u}}), \mathbf{v}\rangle_{(\mathbf{H}^1)^* \times \mathbf{H}^1} , \qquad \mathbf{v} \in \mathbf{H}^1 . \tag{4}$$

As shown for instance in [1], the unilateral contact problem between a viscoelastic body and a rigid foundation has at least one weak solution. In the following, we represent the state of a solution $\mathbf{u}$ of (2) for $t_n, t_{n+1} \in [0,T]$ by

$$\mathbf{u}(t_{n+1}) = \boldsymbol{\Phi}^{t_{n+1},t_n}(\mathbf{u}(t_n), \dot{\mathbf{u}}(t_n)) , \quad \dot{\mathbf{u}}(t_{n+1}) = \dot{\boldsymbol{\Phi}}^{t_{n+1},t_n}(\mathbf{u}(t_n), \dot{\mathbf{u}}(t_n))$$

with the *evolution operator* $\bar{\boldsymbol{\Phi}}^{t_{n+1},t_n} := (\boldsymbol{\Phi}^{t_{n+1},t_n}, \dot{\boldsymbol{\Phi}}^{t_{n+1},t_n}) : \mathbf{H}^1 \times \mathbf{L}^2 \longrightarrow \mathbf{H}^1 \times \mathbf{L}^2$.

2.2 Contact–stabilized Newmark scheme

Here, we turn towards the spatiotemporal discretization of the dynamical contact problem (2). We use the method of time layers (MOT), also known as Rothe method, in which we discretize first in time and then in space.

For integration in time, we consider the contact–stabilized Newmark method (CSN) as suggested by Deuflhard, Krause, and Ertel for the purely elastic case [6]. This scheme is energy dissipative in the presence of contact and avoids the occurrence of artificial numerical oscillations at contact boundaries. The latter feature is achieved by performing a discrete $\mathbf{L}^2$-projection at contact interfaces at each timestep. In [17], the authors have given the generalization of the contact–stabilized Newmark method to the viscoelastic case.

In order to fix notation, let the continuous time interval $[t_0, T]$ be subdivided by $N_{\Delta_\tau}+1$ discrete time points $t_0 < t_1 < \cdots < t_{N_{\Delta_\tau}} = T$ which are forming an equidistant mesh $\Delta_\tau = \{t_0, t_1, \dots, T\}$. The constant timestep is denoted by τ.

Contact–stabilized Newmark method (CSN).

$$
\begin{aligned}
0 &\in \mathbf{u}^{n+1}_{\text{pred}} - \big(\mathbf{u}^n + \tau\dot{\mathbf{u}}^n\big) + \partial I_{\mathcal{K}}\big(\mathbf{u}^{n+1}_{\text{pred}}\big)\\
0 &\in \mathbf{u}^{n+1} - \mathbf{u}^{n+1}_{\text{pred}} + \frac{1}{2}\tau^2\Big(\mathbf{F}\Big(\tfrac{\mathbf{u}^n+\mathbf{u}^{n+1}}{2}\Big) + \mathbf{G}\Big(\tfrac{\mathbf{u}^{n+1}-\mathbf{u}^n}{\tau}\Big) + \partial I_{\mathcal{K}}\big(\mathbf{u}^{n+1}\big)\Big)\\
\dot{\mathbf{u}}^{n+1} &= \dot{\mathbf{u}}^n - \tau\Big(\mathbf{F}\Big(\tfrac{\mathbf{u}^n+\mathbf{u}^{n+1}}{2}\Big) + \mathbf{G}\Big(\tfrac{\mathbf{u}^{n+1}-\mathbf{u}^n}{\tau}\Big) - \mathbf{F}_{\text{con}}\big(\mathbf{u}^{n+1}\big)\Big)
\end{aligned}
\tag{5}
$$

where the contact forces $\mathbf{F}_{\text{con}}\big(\mathbf{u}^{n+1}\big)$ are defined by

$$
\begin{aligned}
&\frac{1}{2}\tau^2\big\langle \mathbf{F}_{\text{con}}\big(\mathbf{u}^{n+1}\big), \mathbf{v}\big\rangle_{(\mathbf{H}^1)^*\times\mathbf{H}^1} \qquad (6)\\
&= \Big\langle \mathbf{u}^{n+1} - \mathbf{u}^{n+1}_{\text{pred}} + \frac{1}{2}\tau^2\Big(\mathbf{F}\Big(\tfrac{\mathbf{u}^n+\mathbf{u}^{n+1}}{2}\Big) + \mathbf{G}\Big(\tfrac{\mathbf{u}^{n+1}-\mathbf{u}^n}{\tau}\Big)\Big), \mathbf{v}\Big\rangle_{(\mathbf{H}^1)^*\times\mathbf{H}^1}, \qquad \mathbf{v}\in\mathbf{H}^1 .
\end{aligned}
$$

We assume that the spatial quantities corresponding to $\mathbf{u}^n$ are obtained via finite elements $\mathbf{S}_h$ with a spatial mesh size parameter $h > 0$. In this setting, $\mathcal{K} \subset \mathbf{S}_h$ has to be understood as a discrete approximation of the set of admissible displacements. For details concerning the spatial discretization, we refer the reader to [14, 18]. The arising constrained minimization problems in space can be solved by adaptive monotone multigrid methods (see [10, 18, 19]).

In analogy to the continuous problem, we define the *discrete evolution operator* $\bar{\mathbf{\Psi}}^{t_{n+1},t_n} := \big(\mathbf{\Psi}^{t_{n+1},t_n}, \dot{\mathbf{\Psi}}^{t_{n+1},t_n}\big) : \mathbf{H}^1\times\mathbf{L}^2 \longrightarrow \mathbf{H}^1\times\mathbf{L}^2$ for $t_n, t_{n+1}\in\Delta_\tau$ via

$$
\mathbf{u}^{n+1} = \mathbf{\Psi}^{t_{n+1},t_n}\big(\mathbf{u}^n, \dot{\mathbf{u}}^n\big), \quad \dot{\mathbf{u}}^{n+1} = \dot{\mathbf{\Psi}}^{t_{n+1},t_n}\big(\mathbf{u}^n, \dot{\mathbf{u}}^n\big).
$$

Moreover, we introduce the *lattice function* $\bar{\mathbf{u}}_\tau := \big(\mathbf{u}_\tau, \dot{\mathbf{u}}_\tau\big) : \Delta_\tau \longrightarrow \mathbf{H}^1\times\mathbf{L}^2$ as

$$
\mathbf{u}_\tau(t_{n+1}) = \mathbf{\Psi}^{t_{n+1},t_n}\big(\mathbf{u}_\tau(t_n), \dot{\mathbf{u}}_\tau(t_n)\big), \quad \dot{\mathbf{u}}_\tau(t_{n+1}) = \dot{\mathbf{\Psi}}^{t_{n+1},t_n}\big(\mathbf{u}_\tau(t_n), \dot{\mathbf{u}}_\tau(t_n)\big)
$$

with

$$
\mathbf{u}_\tau(t_0) = \mathbf{u}^0, \quad \dot{\mathbf{u}}_\tau(t_0) = \dot{\mathbf{u}}^0 .
$$

Remark 2.1. In [17], the authors have proven that the contact–stabilized Newmark method coincides with the modified Newmark scheme by Kane et al. ([13]) in function space. Since we use the method of time layers, the numerical analysis in this paper will cover both Newmark methods simultaneously. Nevertheless, we will restrict our considerations to CSN due to its nice numerical features.

2.3 Sensitivity and consistency results

In Section 3, we will work out an asymptotic error expansion of the contact–stabilized Newmark method. For the convenience of the reader, we recall known results concerning the sensitivity and consistency of the scheme from [17] and [21].

Conical derivative. First of all, we need the well–posedness of CSN with respect to perturbations of the initial data. In [21], an important result has been given which concerns the directional differentiability of the solution $\mathbf{u} = \mathbf{u}(\mathbf{f}) \in \mathcal{K}$ of an elliptic variational inequality

$$a(\mathbf{u}, \mathbf{v} - \mathbf{u}) \geq \langle \mathbf{f}, \mathbf{v} - \mathbf{u} \rangle_{\mathbf{V}^* \times \mathbf{V}}\,, \qquad \forall\, \mathbf{v} \in \mathcal{K}$$

on a Hilbert space $\mathbf{V}$. The convex set $\mathcal{K}$ is of the form $\mathcal{K} = \{\mathbf{w} \in \mathbf{V} \mid \ \mathbf{w} \leq \mathbf{g} \text{ a.e.}\}$ with $\mathbf{g}$ continuous, $a(\cdot,\cdot)$ has to fulfill usual ellipticity and continuity assumptions, and $\mathbf{f} \in \mathbf{V}^*$. Then, the mapping $\mathbf{f} \longrightarrow \mathbf{u}(\mathbf{f})$ has a conical derivative $\mathbf{Du}(\mathbf{f})(\cdot)$ on $\mathbf{V}^*$, and $\mathbf{Du}(\mathbf{f})(\mathbf{w}) \in \tilde{\mathcal{K}}^{\mathbf{u}}$ is the solution of the variational inequality

$$a(\mathbf{Du}(\mathbf{f})(\mathbf{w}), \mathbf{v} - \mathbf{Du}(\mathbf{f})(\mathbf{w})) \geq \langle \mathbf{w}, \mathbf{v} - \mathbf{Du}(\mathbf{f})(\mathbf{w}) \rangle_{\mathbf{V}^* \times \mathbf{V}}\,, \qquad \forall\, \mathbf{v} \in \tilde{\mathcal{K}}^{\mathbf{u}}$$

with a modified admissible set

$$\tilde{\mathcal{K}}^{\mathbf{u}} \;=\; \{\mathbf{w} \in \mathbf{V} \,|\, \mathbf{w} \leq 0 \text{ if } \mathbf{u} = \mathbf{g},\; a(\mathbf{u}, \mathbf{w}) = \langle \mathbf{f}, \mathbf{w} \rangle_{\mathbf{V}^* \times \mathbf{V}}\}\,.$$

The transfer of this result to CSN yields the following sensitivity result.

Theorem 2.2 ([21])**.** *The discrete evolution operator* $\big(\boldsymbol{\Psi}^{t+\tau,t}, \dot{\boldsymbol{\Psi}}^{t+\tau,t}\big)$ *possesses a conical derivative* $\bar{\mathbf{D}}\boldsymbol{\Psi}^{t+\tau,t} := \big(\mathbf{D}\boldsymbol{\Psi}^{t+\tau,t}, \dot{\mathbf{D}}\boldsymbol{\Psi}^{t+\tau,t}\big)$*, i.e.*

$$\boldsymbol{\Psi}^{t+\tau,t}(\bar{\mathbf{u}} + h\bar{\mathbf{w}}) = \boldsymbol{\Psi}^{t+\tau,t}\bar{\mathbf{u}} + h\mathbf{D}\boldsymbol{\Psi}^{t+\tau,t}\bar{\mathbf{u}}(\bar{\mathbf{w}}) + \boldsymbol{\theta}(h, \bar{\mathbf{w}})$$

and

$$\dot{\boldsymbol{\Psi}}^{t+\tau,t}(\bar{\mathbf{u}} + h\bar{\mathbf{w}}) = \dot{\boldsymbol{\Psi}}^{t+\tau,t}\bar{\mathbf{u}} + h\dot{\mathbf{D}}\boldsymbol{\Psi}^{t+\tau,t}\bar{\mathbf{u}}(\bar{\mathbf{w}}) + \frac{2}{\tau}\boldsymbol{\theta}(h, \bar{\mathbf{w}})$$

where

$$\lim_{h \to 0} \|\boldsymbol{\theta}(h, \bar{\mathbf{w}})\|_{\mathbf{H}^1}/h = 0$$

for all $h > 0$ and $\bar{\mathbf{u}} = (\mathbf{u}, \dot{\mathbf{u}})\,, \bar{\mathbf{w}} = (\mathbf{w}, \dot{\mathbf{w}}) \in \mathbf{H}^1 \times \mathbf{L}^2$. The conical derivative is given as the solution of

$$
\begin{aligned}
&0 \in \mathbf{w}_{\mathrm{pred}} - (\mathbf{w} + \tau\dot{\mathbf{w}}) + \partial I_{\tilde{\mathcal{K}}^{\boldsymbol{\Psi}^{t+\tau,t}\bar{\mathbf{u}}}}\big(\mathbf{w}_{\mathrm{pred}}\big)\\
&0 \in \mathbf{D}\boldsymbol{\Psi}^{t+\tau,t}\bar{\mathbf{u}}(\bar{\mathbf{w}}) - \mathbf{w}_{\mathrm{pred}} + \frac{1}{2}\tau^2\Big(\mathbf{F}\Big(\tfrac{\mathbf{w}+\mathbf{D}\boldsymbol{\Psi}^{t+\tau,t}\bar{\mathbf{u}}(\bar{\mathbf{w}})}{2}\Big) + \mathbf{G}\Big(\tfrac{\mathbf{D}\boldsymbol{\Psi}^{t+\tau,t}\bar{\mathbf{u}}(\bar{\mathbf{w}})-\mathbf{w}}{\tau}\Big)\\
&\qquad\qquad\qquad\qquad + \partial I_{\tilde{\mathcal{K}}^{\boldsymbol{\Psi}^{t+\tau,t}\bar{\mathbf{u}}}}\big(\mathbf{D}\boldsymbol{\Psi}^{t+\tau,t}\bar{\mathbf{v}}(\bar{\mathbf{w}})\big)\Big) \qquad (7)\\
&\dot{\mathbf{D}}\boldsymbol{\Psi}^{t+\tau,t}\bar{\mathbf{u}}(\bar{\mathbf{w}}) = \dot{\mathbf{w}} - \tau\Big(\mathbf{F}\Big(\tfrac{\mathbf{w}+\mathbf{D}\boldsymbol{\Psi}^{t+\tau,t}\bar{\mathbf{u}}(\bar{\mathbf{w}})}{2}\Big) + \mathbf{G}\Big(\tfrac{\mathbf{D}\boldsymbol{\Psi}^{t+\tau,t}\bar{\mathbf{u}}(\bar{\mathbf{w}})-\mathbf{w}}{\tau}\Big)\\
&\qquad\qquad - \mathbf{F}_{\mathrm{con}}\big(\mathbf{D}\boldsymbol{\Psi}^{t+\tau,t}\bar{\mathbf{u}}(\bar{\mathbf{w}})\big)\Big)
\end{aligned}
$$

with contact forces

$$
\begin{aligned}
&\frac{1}{2}\tau^2\big\langle\mathbf{F}_{\mathrm{con}}\big(\mathbf{D}\boldsymbol{\Psi}^{t+\tau,t}\bar{\mathbf{u}}(\bar{\mathbf{w}})\big), \mathbf{v}\big\rangle \qquad (8)\\
&= \Big\langle \mathbf{D}\boldsymbol{\Psi}^{t+\tau,t}\bar{\mathbf{u}}(\bar{\mathbf{w}}) - \mathbf{w}_{\mathrm{pred}} + \frac{1}{2}\tau^2\Big(\mathbf{F}\Big(\tfrac{\mathbf{w}+\mathbf{D}\boldsymbol{\Psi}^{t+\tau,t}\bar{\mathbf{u}}(\bar{\mathbf{w}})}{2}\Big) + \mathbf{G}\Big(\tfrac{\mathbf{D}\boldsymbol{\Psi}^{t+\tau,t}\bar{\mathbf{u}}(\bar{\mathbf{w}})-\mathbf{w}}{\tau}\Big)\Big), \mathbf{v}\Big\rangle
\end{aligned}
$$

for $\mathbf{v} \in \mathbf{H}^1$ and

$$
\tilde{\mathcal{K}}^{\boldsymbol{\Psi}^{t+\tau,t}\bar{\mathbf{u}}} = \big\{\mathbf{w} \in \mathbf{H}^1_D \,\big|\, [\mathbf{w}\cdot\boldsymbol{\nu}]_\phi \le 0 \text{ if } \big[\boldsymbol{\Psi}^{t+\tau,t}\bar{\mathbf{u}}\cdot\boldsymbol{\nu}\big]_\phi = g,\ \big\langle\mathbf{F}_{\mathrm{con}}\big(\boldsymbol{\Psi}^{t+\tau,t}\bar{\mathbf{u}}\big), \mathbf{w}\big\rangle = 0\big\}\,. \qquad (9)
$$

The conical derivative is defined via CSN on a modified admissible set $\tilde{\mathcal{K}}^{\boldsymbol{\Psi}^{t+\tau,t}\bar{\mathbf{u}}}$. Strict complementarity implies that $[\mathbf{D}\boldsymbol{\Psi}^{t+\tau,t}\bar{\mathbf{u}}(\bar{\mathbf{w}})\cdot\boldsymbol{\nu}]_\phi = 0$ on those parts of the possible contact boundaries where $[\boldsymbol{\Psi}^{t+\tau,t}\bar{\mathbf{u}}\cdot\boldsymbol{\nu}]_\phi = g$. Then, the variational inclusion in the second line of the scheme reduces to a minimization problem with time-dependent Dirichlet boundaries. The theorem does not give any information about the sensitivity of CSN in the special case of interest where h coincides with the parameter τ.

Remark. A simple calculation shows that

$$
\dot{\mathbf{D}}\boldsymbol{\Psi}^{t+\tau,t}\bar{\mathbf{u}}(\bar{\mathbf{w}}) = \dot{\mathbf{w}} + \frac{2}{\tau}\big(\mathbf{D}\boldsymbol{\Psi}^{t+\tau,t}\bar{\mathbf{u}}(\bar{\mathbf{w}}) - \mathbf{w}_{\mathrm{pred}}\big)\,.
$$

In [17], the authors have proven that the predictor $\mathbf{w}_{\mathrm{pred}}$ resulting from a $\mathbf{L}^2$-projection converges to $\mathbf{w} + \tau\dot{\mathbf{w}}$ if the spatial discretization parameter h tends to zero. Hence, we find the relation

$$
\dot{\mathbf{D}}\boldsymbol{\Psi}^{t+\tau,t}\bar{\mathbf{u}}(\bar{\mathbf{w}}) = -\dot{\mathbf{w}} + \frac{2}{\tau}\big(\mathbf{D}\boldsymbol{\Psi}^{t+\tau,t}\bar{\mathbf{u}}(\bar{\mathbf{w}}) - \mathbf{w}\big) \qquad (10)
$$

in function space.

Physical energy norm. In [16], the authors introduced a mix of norms in function space which allows to prove a perturbation result for a class of dynamical contact problems of type (2). For a function $\bar{\mathbf{v}} = (\mathbf{v}, \dot{\mathbf{v}}) : [t, t+\tau] \to \mathbf{H}^1 \times \mathbf{L}^2$ with $\dot{\mathbf{v}} \in \mathbf{L}^2(t, t+\tau, \mathbf{H}^1)$, we define

$$\|\bar{\mathbf{v}}\|^2_{\mathcal{E}(t,\tau)} := \|\bar{\mathbf{v}}(t+\tau)\|^2_E + \int_t^{t+\tau} \big\|\dot{\mathbf{v}}(s)\big\|^2_b \, ds \tag{11}$$

in terms of

$$\|\bar{\mathbf{v}}(t+\tau)\|^2_E := \frac{1}{2}\big\|\dot{\mathbf{v}}(t+\tau)\big\|^2_{\mathbf{L}^2} + \frac{1}{2}\big\|\mathbf{v}(t+\tau)\big\|^2_a \,. \tag{12}$$

The physical energy norm may be interpreted as the sum of the kinetic energy, the potential energy, and the viscoelastic part.

Consistency error. In [17], the authors derived an estimate for the consistency error of the classical Newmark method, the modified Newmark method by Kane et al., and CSN within the physical energy norm

$$\begin{aligned}\big\|\bar{\mathbf{\Psi}} - \bar{\mathbf{\Phi}}\big\|^2_{\mathcal{E}(t,\tau)} := &\frac{1}{2}\big\|\dot{\mathbf{\Psi}}^{t+\tau,t}\bar{\mathbf{u}}(t) - \dot{\mathbf{\Phi}}^{t+\tau,t}\bar{\mathbf{u}}(t)\big\|^2_{\mathbf{L}^2} + \frac{1}{2}\big\|\mathbf{\Psi}^{t+\tau,t}\bar{\mathbf{u}}(t) - \mathbf{\Phi}^{t+\tau,t}\bar{\mathbf{u}}(t)\big\|^2_a \\ &+ \int_t^{t+\tau} \bigg\|\frac{\mathbf{\Psi}^{t+s,t}\bar{\mathbf{u}}(t) - \mathbf{u}(t)}{\tau} - \dot{\mathbf{\Phi}}^{t+s,t}\bar{\mathbf{u}}(t)\bigg\|^2_b \, ds \,.\end{aligned}$$

In the presence of contact, this result requires the solution of the dynamical contact problem together with its first and second derivative to be in the function space of bounded variation.

Theorem 2.3 ([17]). *Let $\dot{\mathbf{u}} \in \mathrm{BV}\big([t, t+\tau], \mathbf{H}^1\big)$ and $\ddot{\mathbf{u}} \in \mathrm{BV}\big([t, t+\tau], (\mathbf{H}^1)^*\big)$. Then, for initial values $\mathbf{u}^n = \mathbf{u}(t)$ and $\dot{\mathbf{u}}^n = \dot{\mathbf{u}}(t)$, the consistency error of CSN in terms of $\bar{\mathbf{\Psi}} = (\mathbf{\Psi}, \dot{\mathbf{\Psi}})$ satisfies*

$$\big\|\bar{\mathbf{\Psi}} - \bar{\mathbf{\Phi}}\big\|_{\mathcal{E}(t,\tau)} = R(\mathbf{u}, [t, t+\tau]) \cdot O\big(\tau^{1/2}\big)$$

where

$$\begin{aligned} R(\mathbf{u}, [t, t+\tau]) := &\,\mathrm{TV}\big(\mathbf{u}, [t, t+\tau], \mathbf{H}^1\big) + \mathrm{TV}\big(\dot{\mathbf{u}}, [t, t+\tau], \mathbf{H}^1\big) \\ &+ \mathrm{TV}\big(\ddot{\mathbf{u}}, [t, t+\tau], (\mathbf{H}^1)^*\big) \,. \end{aligned} \tag{13}$$

The formulation of the consistency result in function space does not give any information about the spatial distribution of the consistency error of CSN. Analyzing the proof of the theorem as presented in [17], we find that the estimate can be improved if the active contact boundaries do not change during the timestep. This result will be verified in detail in a PhD thesis [15].

A central role for the construction of an adaptive timestep control is played by the choice of norm in which the approximation error of the scheme is measured.

The existing perturbation and consistency results for CSN suggest to use the full physical energy norm $\|\cdot\|_{\mathcal{E}}$. In the absence of contact, the Newmark scheme has pointwise the consistency order 2 in positions as well as velocities. Hence, due to the integral over time, the viscoelastic part of the physical energy norm is of higher order than the kinetic and potential parts. In view of an adaptive timestep control, we neglect the viscoelastic part, and we are only interested in the reduced physical energy norm $\|\cdot\|_E$.

3 Towards an asymptotic error expansion

The main challenge for an adaptive timestep control is the construction of a suitable error estimator. Usually, the numerical integrator of interest is compared to a second, higher order discrete evolution. We want to construct such a scheme by means of extrapolation techniques which are based on an asymptotic error expansion. The scope of this section is to analyze the existence of such an error representation for the contact–stabilized Newmark method.

3.1 Extension of extrapolation techniques

For ordinary differential equations, a proof technique for an asymptotic error expansion can be found in [11]. Here, we will extend this approach to dynamical contact problems.

We define a discrete evolution $\bar{\mathbf{\Psi}}_*^{t+\tau,t} := (\mathbf{\Psi}_*^{t+\tau,t}, \dot{\mathbf{\Psi}}_*^{t+\tau,t}) : \mathbf{H}^1 \times \mathbf{L}^2 \longrightarrow \mathbf{H}^1 \times \mathbf{L}^2$ via the formulas

$$\begin{aligned} \mathbf{\Psi}_*^{t+\tau,t}\bar{\mathbf{u}}(t) &:= \mathbf{\Psi}^{t+\tau,t}(\bar{\mathbf{u}}(t) + \bar{\mathbf{e}}(t)\tau^p) - \mathbf{e}(t+\tau)\tau^p \\ \dot{\mathbf{\Psi}}_*^{t+\tau,t}\bar{\mathbf{u}}(t) &:= \dot{\mathbf{\Psi}}^{t+\tau,t}(\bar{\mathbf{u}}(t) + \bar{\mathbf{e}}(t)\tau^p) - \boldsymbol{\epsilon}(t+\tau)\tau^p\,. \end{aligned} \tag{14}$$

For fixed initial time t_0, the functions $\bar{\mathbf{e}} := (\mathbf{e}, \boldsymbol{\epsilon}) : [t_0, T] \to \mathbf{H}^1 \times \mathbf{L}^2$ should have initial values equal to zero, i.e.

$$\mathbf{e}(t_0) = 0\,, \quad \boldsymbol{\epsilon}(t_0) = 0\,. \tag{15}$$

We will specify these functions in Section 3.2 below. For constant stepsize τ, the lattice function $\bar{\mathbf{u}}_\tau^* = (\mathbf{u}_\tau^*, \dot{\mathbf{u}}_\tau^*) : \Delta_\tau \longrightarrow \mathbf{H}^1 \times \mathbf{L}^2$ of the new evolution correlates with the one of CSN in the following way.

Lemma 3.1. *For $t \in \Delta_\tau$, the lattice functions $(\mathbf{u}_\tau^*, \dot{\mathbf{u}}_\tau^*)$ and $(\mathbf{u}_\tau, \dot{\mathbf{u}}_\tau)$ satisfy the relation*

$$\begin{aligned} \mathbf{u}_\tau(t) - \mathbf{u}(t) - \mathbf{e}(t)\tau^p &= \mathbf{u}_\tau^*(t) - \mathbf{u}(t) \\ \dot{\mathbf{u}}_\tau(t) - \dot{\mathbf{u}}(t) - \boldsymbol{\epsilon}(t)\tau^p &= \dot{\mathbf{u}}_\tau^*(t) - \dot{\mathbf{u}}(t)\,. \end{aligned}$$

Proof. Due to definition (14) with initial values (15), we find

$$\bar{\mathbf{u}}_\tau^*(t_0+\tau) = \bar{\mathbf{\Psi}}^{t_0+\tau,t_0}(\bar{\mathbf{u}}(t_0) + \bar{\mathbf{e}}(t_0)\tau^p) - \bar{\mathbf{e}}(t_0+\tau)\tau^p = \bar{\mathbf{u}}_\tau(t_0+\tau) - \bar{\mathbf{e}}(t_0+\tau)\tau^p\,.$$

An induction leads to

$$\bar{\mathbf{u}}^*_\tau(t) = \bar{\mathbf{\Psi}}^{t,t-\tau}(\bar{\mathbf{u}}^*_\tau(t-\tau) + \bar{\mathbf{e}}(t-\tau)\tau^p) - \bar{\mathbf{e}}(t)\tau^p = \bar{\mathbf{u}}_\tau(t) - \bar{\mathbf{e}}(t)\tau^p$$

which gives the desired relation. □

The lemma yields an asymptotic error expansion of order p for CSN if the approximation error $\bar{\mathbf{u}}^*_\tau - \bar{\mathbf{u}}$ of the new scheme is of order $o(\tau^p)$. In order to gain more information on this quantity, we consider the error of the scheme after performing two timesteps with stepsize $\tau/2$, for simplicity. The global error of a numerical integration is based on the continuous dependence of the scheme on the initial data.

Assumption 3.2. Let CSN fulfill

$$\left\|\bar{\mathbf{\Psi}}^{t+\tau,t}\bar{\mathbf{u}}(t) - \bar{\mathbf{\Psi}}^{t+\tau,t}\bar{\tilde{\mathbf{u}}}(t)\right\|_E \leq C_p \cdot \left\|\bar{\mathbf{u}}(t) - \bar{\tilde{\mathbf{u}}}(t)\right\|_E$$

with a constant $C_p > 0$.

In [16], the validity of the continuous analogon of this perturbation result has been proven for a certain class of dynamical contact problems. The discrete perturbation behavior will be discussed in a PhD thesis [15]. Now, we can prove an estimate for the approximation error of the new scheme $(\mathbf{\Psi}_*, \dot{\mathbf{\Psi}}_*)$.

Theorem 3.3. *Let Assumption* 3.2 *hold. Then,*

$$\begin{aligned}&\left\|\bar{\mathbf{u}}^*_{\frac{\tau}{2}}(t+\tau) - \bar{\mathbf{u}}(t+\tau)\right\|_E \\ &\leq C_p \cdot \left\|\left(\bar{\mathbf{\Psi}}_*^{t+\frac{\tau}{2},t} - \bar{\mathbf{\Phi}}^{t+\frac{\tau}{2},t}\right)\bar{\mathbf{u}}(t)\right\|_E + \left\|\left(\bar{\mathbf{\Psi}}_*^{t+\tau,t+\frac{\tau}{2}} - \bar{\mathbf{\Phi}}^{t+\tau,t+\frac{\tau}{2}}\right)\bar{\mathbf{u}}\left(t+\frac{\tau}{2}\right)\right\|_E.\end{aligned}$$

Proof. The error of a numerical scheme after performing two timesteps can be divided into the consistency error of the second step and the propagation of the consistency error of the first step, i.e.

$$\begin{aligned}&\bar{\mathbf{u}}^*_{\frac{\tau}{2}}(t+\tau) - \bar{\mathbf{u}}(t+\tau) \\ &= \bar{\mathbf{\Psi}}_*^{t+\tau,t+\frac{\tau}{2}}\bar{\mathbf{\Psi}}_*^{t+\frac{\tau}{2},t}\bar{\mathbf{u}}(t) - \bar{\mathbf{\Phi}}^{t+\tau,t+\frac{\tau}{2}}\bar{\mathbf{\Phi}}^{t+\frac{\tau}{2},t}\bar{\mathbf{u}}(t) \\ &= \bar{\mathbf{\Psi}}_*^{t+\tau,t+\frac{\tau}{2}}\bar{\mathbf{\Psi}}_*^{t+\frac{\tau}{2},t}\bar{\mathbf{u}}(t) - \bar{\mathbf{\Psi}}_*^{t+\tau,t+\frac{\tau}{2}}\bar{\mathbf{\Phi}}^{t+\frac{\tau}{2},t}\bar{\mathbf{u}}(t) + \left(\bar{\mathbf{\Psi}}_*^{t+\tau,t+\frac{\tau}{2}} - \bar{\mathbf{\Phi}}^{t+\tau,t+\frac{\tau}{2}}\right)\bar{\mathbf{u}}\left(t+\frac{\tau}{2}\right).\end{aligned}$$

Due to definitions (14)–(15) and Assumption 3.2, we find for the propagated consistency error

$$\begin{aligned}&\left\|\bar{\mathbf{\Psi}}_*^{t+\tau,t+\frac{\tau}{2}}\bar{\mathbf{\Psi}}_*^{t+\frac{\tau}{2},t}\bar{\mathbf{u}}(t) - \bar{\mathbf{\Psi}}_*^{t+\tau,t+\frac{\tau}{2}}\bar{\mathbf{\Phi}}^{t+\frac{\tau}{2},t}\bar{\mathbf{u}}(t)\right\|_E \\ &= \left\|\bar{\mathbf{\Psi}}^{t+\tau,t+\frac{\tau}{2}}\bar{\mathbf{\Psi}}^{t+\frac{\tau}{2},t}\bar{\mathbf{u}}(t) - \bar{\mathbf{\Psi}}^{t+\tau,t+\frac{\tau}{2}}\left(\bar{\mathbf{\Phi}}^{t+\frac{\tau}{2},t}\bar{\mathbf{u}}(t) + \bar{\mathbf{e}}\left(t+\frac{\tau}{2}\right)\left(\frac{\tau}{2}\right)^p\right)\right\|_E \\ &\leq C_p \cdot \left\|\bar{\mathbf{\Psi}}^{t+\frac{\tau}{2},t}\bar{\mathbf{u}}(t) - \left(\bar{\mathbf{\Phi}}^{t+\frac{\tau}{2},t}\bar{\mathbf{u}}(t) + \bar{\mathbf{e}}\left(t+\frac{\tau}{2}\right)\left(\frac{\tau}{2}\right)^p\right)\right\|_E \\ &= C_p \cdot \left\|\left(\bar{\mathbf{\Psi}}_*^{t+\frac{\tau}{2},t} - \bar{\mathbf{\Phi}}^{t+\frac{\tau}{2},t}\right)\bar{\mathbf{u}}(t)\right\|_E.\end{aligned}$$

This gives the estimate of the theorem. □

In view of an asymptotic error expansion of CSN, we combine the results of Lemma 3.1 and Theorem 3.3. This yields that we have to construct the functions $(\mathbf{e}, \boldsymbol{\epsilon})$ such that

$$\frac{\left\|\bar{\boldsymbol{\Psi}}_*^{t+\tau,t} - \bar{\boldsymbol{\Phi}}^{t+\tau,t}\right\|_E}{\left\|\bar{\boldsymbol{\Psi}}^{t+\tau,t} - \bar{\boldsymbol{\Phi}}^{t+\tau,t}\right\|_E} \to 0 \quad \text{for } \tau \to 0\,, \tag{16}$$

i.e. the consistency error of $(\boldsymbol{\Psi}_*, \dot{\boldsymbol{\Psi}}_*)$ in energy norm should be of higher order than the one of CSN for arbitrary initial times.

3.2 Construction of a higher order scheme

The task of this section is to find a definition for the functions $(\mathbf{e}, \boldsymbol{\epsilon})$ such that the initial values (15) and condition (16) on the consistency error of the new scheme are fulfilled. For this purpose, we need information about the pointwise error behavior of CSN. While such information is given in the absence of contact, up to now, the only consistency result for CSN in the presence of contact is given in energy norm (cf. Theorem 2.3). Hence, we lay the following analysis of an asymptotic error expansion of CSN on a very general basis.

Assumption 3.4. Let the consistency error of CSN be of the form

$$\begin{aligned} \boldsymbol{\Psi}^{t+\tau,t}\bar{\mathbf{u}} - \boldsymbol{\Phi}^{t+\tau,t}\bar{\mathbf{u}} &= \mathbf{m}(t)\cdot\tau^{p+1} + \mathbf{r}(t,\tau)\cdot\tau^p \\ \dot{\boldsymbol{\Psi}}^{t+\tau,t}\bar{\mathbf{u}} - \dot{\boldsymbol{\Phi}}^{t+\tau,t}\bar{\mathbf{u}} &= \int_t^{t+\tau}\boldsymbol{\mu}(s)\,ds\cdot\tau^p + \boldsymbol{\rho}(t,\tau)\cdot\tau^p \end{aligned} \tag{17}$$

with $\mathbf{m} \in C([0,T],\mathbf{H}^1)$ and $\dot{\mathbf{m}}, \boldsymbol{\mu} \in \mathbf{W}^{1,2}(0,T;\mathbf{H}^1,\mathbf{L}^2)$.

In the following, we will often use the abbreviation $\bar{\mathbf{m}} := (\mathbf{m}, \boldsymbol{\mu})$. Please note that the second line of Assumption 3.4 is not the derivative of the first one due to the definition of the discrete evolution operator. The integral term in the consistency error of the velocities is related to the viscoelastic part of the physical energy norm. In the classical approach, we would expect a pointwise Taylor expansion of the consistency error of the scheme. This is included in our ansatz if

$$\int_t^{t+\tau}\boldsymbol{\mu}(s)\,ds = \boldsymbol{\mu}(t)\cdot\tau + o(\tau)$$

and

$$|\mathbf{r}(t,\tau)| = o(\tau)\,, \quad |\boldsymbol{\rho}(t,\tau)| = o(\tau)\,.$$

For a perturbation of the initial values of CSN, we write

$$\begin{aligned} \boldsymbol{\Psi}^{t+\tau,t}(\bar{\mathbf{u}} + \bar{\mathbf{e}}\tau^p) - \boldsymbol{\Psi}^{t+\tau,t}\bar{\mathbf{u}} &= \left(\mathbf{D}\boldsymbol{\Psi}^{t+\tau,t}\bar{\mathbf{u}}(\bar{\mathbf{e}}) + \mathbf{p}(t,\tau)\right)\cdot\tau^p \\ \dot{\boldsymbol{\Psi}}^{t+\tau,t}(\bar{\mathbf{u}} + \bar{\mathbf{e}}\tau^p) - \dot{\boldsymbol{\Psi}}^{t+\tau,t}\bar{\mathbf{u}} &= \left(\dot{\mathbf{D}}\boldsymbol{\Psi}^{t+\tau,t}\bar{\mathbf{u}}(\bar{\mathbf{e}}) + \boldsymbol{\pi}(t,\tau)\right)\cdot\tau^p \end{aligned} \tag{18}$$

where $(\mathbf{D}\boldsymbol{\Psi}^{t+\tau,t}\bar{\mathbf{u}}(\bar{\mathbf{e}}), \dot{\mathbf{D}}\boldsymbol{\Psi}^{t+\tau,t}\bar{\mathbf{u}}(\bar{\mathbf{e}}))$ denotes the conical derivative of the scheme introduced in Section 2.3. A short calculation shows that $\boldsymbol{\pi}(t,\tau) = \frac{2}{\tau}\mathbf{p}(t,\tau)$, and we will often use the notation $\bar{\mathbf{p}} := (\mathbf{p}, \boldsymbol{\pi})$. We expect that $\mathbf{p}(t,\tau)$ and $\boldsymbol{\pi}(t,\tau)$ are of order $o(\tau)$. In the case of time-constant Dirichlet boundaries, the variational problem is linear and $|\bar{\mathbf{p}}(t,\tau)| = 0$.

On the basis of these notations, we present a formula for the consistency error of the new evolution $(\boldsymbol{\Psi}_*, \dot{\boldsymbol{\Psi}}_*)$.

Lemma 3.5. *Let Assumption* 3.4 *hold. Then, the consistency error in terms of the discrete evolution* $\bar{\boldsymbol{\Psi}}_* = (\boldsymbol{\Psi}_*, \dot{\boldsymbol{\Psi}}_*)$ *satisfies*

$$\begin{aligned}
\boldsymbol{\Psi}_*^{t+\tau,t}\bar{\mathbf{u}}(t) - \boldsymbol{\Phi}^{t+\tau,t}\bar{\mathbf{u}}(t) &= \big(\mathbf{D}\boldsymbol{\Psi}^{t+\tau,t}\bar{\mathbf{u}}(t)(\bar{\mathbf{e}}(t)) - \mathbf{e}(t+\tau) + \tau\mathbf{m}(t)\big)\cdot\tau^p \\
&\quad + (\mathbf{r}(t,\tau) + \mathbf{p}(t,\tau))\cdot\tau^p \\
\dot{\boldsymbol{\Psi}}_*^{t+\tau,t}\bar{\mathbf{u}}(t) - \dot{\boldsymbol{\Phi}}^{t+\tau,t}\bar{\mathbf{u}}(t) &= \Big(\dot{\mathbf{D}}\boldsymbol{\Psi}^{t+\tau,t}\bar{\mathbf{u}}(t)(\bar{\mathbf{e}}(t)) - \boldsymbol{\epsilon}(t+\tau) + \int_t^{t+\tau}\boldsymbol{\mu}(s)\,ds\Big)\cdot\tau^p \\
&\quad + (\boldsymbol{\rho}(t,\tau) + \boldsymbol{\pi}(t,\tau))\cdot\tau^p\,.
\end{aligned}$$

Proof. Inserting definition (14) into the consistency error yields

$$\bar{\boldsymbol{\Psi}}_*^{t+\tau,t}\bar{\mathbf{u}}(t) - \bar{\boldsymbol{\Phi}}^{t+\tau,t}\bar{\mathbf{u}}(t) = \bar{\boldsymbol{\Psi}}^{t+\tau,t}(\bar{\mathbf{u}}(t) + \bar{\mathbf{e}}(t)\tau^p) - \bar{\mathbf{e}}(t+\tau)\tau^p - \bar{\boldsymbol{\Phi}}^{t+\tau,t}\bar{\mathbf{u}}(t)\,.$$

Due to Assumption 3.4 on the consistency error of CSN, we find

$$\begin{aligned}
\bar{\boldsymbol{\Psi}}_*^{t+\tau,t}\bar{\mathbf{u}}(t) - \bar{\boldsymbol{\Phi}}^{t+\tau,t}\bar{\mathbf{u}}(t) &= \bar{\boldsymbol{\Psi}}^{t+\tau,t}(\bar{\mathbf{u}}(t) + \bar{\mathbf{e}}(t)\tau^p) - \bar{\boldsymbol{\Psi}}^{t+\tau,t}\bar{\mathbf{u}}(t) - \bar{\mathbf{e}}(t+\tau)\cdot\tau^p \\
&\quad + \bar{\mathbf{m}}(t)\cdot\tau^{p+1} + \bar{\mathbf{r}}(t,\tau)\cdot\tau^p\,.
\end{aligned}$$

Using (18), we end up with

$$\begin{aligned}
\bar{\boldsymbol{\Psi}}_*^{t+\tau,t}\bar{\mathbf{u}}(t) - \bar{\boldsymbol{\Phi}}^{t+\tau,t}\bar{\mathbf{u}}(t) &= \big(\bar{\mathbf{D}}\boldsymbol{\Psi}^{t+\tau,t}\bar{\mathbf{u}}(t)(\bar{\mathbf{e}}(t)) - \bar{\mathbf{e}}(t+\tau) + \tau\bar{\mathbf{m}}(t)\big)\cdot\tau^p \\
&\quad + (\bar{\mathbf{r}}(t,\tau) + \bar{\mathbf{p}}(t,\tau))\cdot\tau^p\,.
\end{aligned}$$

□

Our aim is to define the functions $(\mathbf{e}, \boldsymbol{\epsilon})$ such that the terms of order $p+1$ in the consistency error of $(\boldsymbol{\Psi}_*, \dot{\boldsymbol{\Psi}}_*)$ vanish, and the scheme is of higher order $o(\tau^{p+1})$. This leads us to the following definition of the functions $(\mathbf{e}, \boldsymbol{\epsilon})$.

Variational problem for $(\mathbf{e}, \boldsymbol{\epsilon})$. For almost every $t \in [t_0, T]$, find $\mathbf{e}(\cdot, t) \in \tilde{\mathcal{K}}^{\mathbf{u}(t)}$ with $\mathbf{e} \in C\big([t_0,T], \mathbf{H}^1\big)$ and $\dot{\mathbf{e}} \in \mathbf{W}^{1,2}\big(t_0, T; \mathbf{H}^1, \mathbf{L}^2\big)$ such that for all $\mathbf{v}(t) \in \tilde{\mathcal{K}}^{\mathbf{u}(t)}$

$$\langle \ddot{\mathbf{e}} - \boldsymbol{\mu} - \dot{\mathbf{m}} + \mathbf{F}(\mathbf{e}) + \mathbf{G}(\dot{\mathbf{e}} - \mathbf{m}), \mathbf{v} - \mathbf{e}\rangle_{(\mathbf{H}^1)^*\times\mathbf{H}^1} \geq 0 \tag{19}$$

and

$$\mathbf{e}(t_0) = 0\,, \quad \dot{\mathbf{e}}(t_0) = \mathbf{m}(t_0) \tag{20}$$

where

$$\tilde{\mathcal{K}}^{\mathbf{u}(t)} = \big\{\mathbf{w} \in \mathbf{H}^1_D \,\big|\, [\mathbf{w}\cdot\boldsymbol{\nu}]_\phi \leq 0 \text{ if } [\mathbf{u}(t)\cdot\boldsymbol{\nu}]_\phi = g,\ \langle \mathbf{F}_{\mathrm{con}}(\mathbf{u}(t)), \mathbf{w}\rangle_{(\mathbf{H}^1)^*\times\mathbf{H}^1} = 0\big\}\,. \tag{21}$$

Further, we set

$$\boldsymbol{\epsilon}(t) = \dot{\mathbf{e}}(t) - \mathbf{m}(t)\,, \qquad \forall\, t \in [t_0, T] \tag{22}$$

such that the initial values (15) are fulfilled. The contact forces $\mathbf{F}_{\mathrm{con}}(\mathbf{e}) \in (\mathbf{H}^1)^*$ are given by

$$\langle \mathbf{F}_{\mathrm{con}}(\mathbf{e}), \mathbf{v}\rangle_{(\mathbf{H}^1)^* \times \mathbf{H}^1} = \langle \ddot{\mathbf{e}} - \boldsymbol{\mu} - \dot{\mathbf{m}} + \mathbf{F}(\mathbf{e}) + \mathbf{G}(\dot{\mathbf{e}} - \mathbf{m}), \mathbf{v}\rangle_{(\mathbf{H}^1)^* \times \mathbf{H}^1}\,, \quad \mathbf{v} \in \mathbf{H}^1\,. \tag{23}$$

In the case of strict complementarity, we find a parabolic equality with Dirichlet boundaries which are varying in time. These boundaries correspond to the active contact boundaries of the solution of the original variational inequality (2). Hence, we assume that $\mathbf{e}$ and its derivatives are of bounded variation in the same sense.

Assumption 3.6. Let the solution of (19) satisfy

$$\dot{\mathbf{e}} \in \mathrm{BV}\big([t, t+\tau], \mathbf{H}^1\big)\,, \quad \ddot{\mathbf{e}} \in \mathrm{BV}\big([t, t+\tau], (\mathbf{H}^1)^*\big)\,.$$

This leads to an estimate for the consistency error of the new evolution $(\boldsymbol{\Psi}_*, \dot{\boldsymbol{\Psi}}_*)$.

Lemma 3.7. *Let Assumptions* 3.4 *and* 3.6 *hold. Then, the consistency error in terms of the discrete evolution* $\bar{\boldsymbol{\Psi}}_* = (\boldsymbol{\Psi}_*, \dot{\boldsymbol{\Psi}}_*)$ *satisfies*

$$\begin{aligned}
&\Big(\Big\| \bar{\boldsymbol{\Psi}}_*^{t+\tau,t} \bar{\mathbf{u}}(t) - \bar{\boldsymbol{\Phi}}^{t+\tau,t} \bar{\mathbf{u}}(t) - (\bar{\mathbf{r}}(t,\tau) + \bar{\mathbf{p}}(t,\tau)) \cdot \tau^p \Big\|_E^2 \\
&\quad + \frac{\tau}{4} \Big\| \dot{\mathbf{D}}\boldsymbol{\Psi}^{t+\tau,t} \bar{\mathbf{u}}(t)(\bar{\mathbf{e}}(t)) - \boldsymbol{\epsilon}(t+\tau) + \int_t^{t+\tau} \boldsymbol{\mu}(s)\, ds \Big\|_b^2 \cdot \tau^{2p} \Big)^{1/2} \\
&\leq \Big(\frac{1}{2} \Big| \Big\langle \mathbf{F}_{\mathrm{con}}\big(\mathbf{D}\boldsymbol{\Psi}^{t+\tau,t} \bar{\mathbf{u}}(t)(\bar{\mathbf{e}}(t))\big) - \mathbf{F}_{\mathrm{con}}(\mathbf{e}(t)), \\
&\qquad \dot{\mathbf{D}}\boldsymbol{\Psi}^{t+\tau,t} \bar{\mathbf{u}}(t)(\bar{\mathbf{e}}(t)) - \boldsymbol{\epsilon}(t+\tau) + \int_t^{t+\tau} \boldsymbol{\mu}(s)\, ds \Big\rangle_{(\mathbf{H}^1)^* \times \mathbf{H}^1} \Big| \Big)^{1/2} \cdot \tau^{p+1/2} \\
&\quad + R(\mathbf{e}, [t, t+\tau]) \cdot O\big(\tau^{p+1/2}\big) + o\big(\tau^{p+1}\big)
\end{aligned} \tag{24}$$

with $R(\mathbf{e}, [t, t+\tau])$ *defined in* (13).

Remark 3.8. Due to the definition of the modified admissible sets (9) and (21), the first term on the right-hand side of (24) can be written as a linear functional on the part of the possible contact boundaries where $\boldsymbol{\Psi}^{t+\tau,t}\bar{\mathbf{u}}(t)$ and $\mathbf{u}(t)$ are actually in contact. Moreover, $\dot{\mathbf{D}}\boldsymbol{\Psi}^{t+\tau,t}\bar{\mathbf{u}}(t)(\bar{\mathbf{e}}(t)) - \boldsymbol{\epsilon}(t+\tau)$ is zero on the part of the contact boundaries where the active sets of $\boldsymbol{\Psi}^{t+\tau,t}\bar{\mathbf{u}}(t)$ and $\mathbf{u}(t+\tau)$ are unchanged and coincide with those of $\mathbf{u}(t)$. This is the same part of the contact boundaries on which we may assume that $\int_t^{t+\tau} \boldsymbol{\mu}(s)\, ds$ is zero by its definition as the consistency error of CSN. Hence, the contact term in the estimate (24) is only effective on a small part of the possible contact boundaries, namely where the active sets vary in time. For most initial times t, this part tends to a set of measure zero as $\tau \to 0$. This effect will also become visible in our numerical examples of Section 3.3 and Section 5.

The localization of the contact stresses on the critical part of the possible contact boundaries is rather tedious without yielding further insight. In [16], a similar argumentation has been worked out in detail. Hence, we leave it at this heuristic discussion. Instead, we will use a rough estimate for the contact term on the right-hand side of (24) in our main theorem.

Proof. By means of Lemma 3.5, the physical energy norm of the consistency error is of the form

$$\begin{aligned} &\big\|\bar{\mathbf{\Psi}}_*^{t+\tau,t}\bar{\mathbf{u}}(t) - \bar{\mathbf{\Phi}}^{t+\tau,t}\bar{\mathbf{u}}(t) - (\bar{\mathbf{r}}(t,\tau)+\bar{\mathbf{p}}(t,\tau))\cdot\tau^p\big\|_E^2 \\ &= \Big(\frac{1}{2}\Big\|\dot{\mathbf{D}}\mathbf{\Psi}^{t+\tau,t}\bar{\mathbf{u}}(t)(\bar{\mathbf{e}}(t)) - \boldsymbol{\epsilon}(t+\tau) + \int_t^{t+\tau}\boldsymbol{\mu}(s)\,ds\Big\|_{\mathbf{L}^2}^2 \\ &\qquad + \frac{1}{2}\big\|\mathbf{D}\mathbf{\Psi}^{t+\tau,t}\bar{\mathbf{u}}(t)(\bar{\mathbf{e}}(t)) - \mathbf{e}(t+\tau) + \tau\mathbf{m}(t)\big\|_a^2\Big)\cdot\tau^{2p}\,. \end{aligned} \tag{25}$$

We want to insert the defining equations for $\mathbf{e}$ and $\boldsymbol{\epsilon}$ into this estimate. For ease of presentation, we introduce the abbreviation

$$\mathbf{v} := \dot{\mathbf{D}}\mathbf{\Psi}^{t+\tau,t}\bar{\mathbf{u}}(t)(\bar{\mathbf{e}}(t)) - \boldsymbol{\epsilon}(t+\tau) + \int_t^{t+\tau}\boldsymbol{\mu}(s)\,ds\,.$$

Since $\dot{\mathbf{e}}, \dot{\mathbf{m}} \in \mathbf{L}^2(t,t+\tau;\mathbf{H}^1)$, we can apply integration by parts. Using the relations (10) and (22), the term in a-seminorm can be written as

$$\begin{aligned} &\mathbf{D}\mathbf{\Psi}^{t+\tau,t}\bar{\mathbf{u}}(t)(\bar{\mathbf{e}}(t)) - \mathbf{e}(t+\tau) + \tau\mathbf{m}(t) \\ &= \frac{\tau}{2}\big(\dot{\mathbf{D}}\mathbf{\Psi}^{t+\tau,t}\bar{\mathbf{u}}(t)(\bar{\mathbf{e}}(t)) + \boldsymbol{\epsilon}(t)\big) - \int_t^{t+\tau}\dot{\mathbf{e}}(s)\,ds + \tau\mathbf{m}(t) \\ &= \frac{\tau}{2}\mathbf{v} + \int_t^{t+\tau}\frac{\boldsymbol{\epsilon}(t+\tau)+\boldsymbol{\epsilon}(t)}{2} - \dot{\mathbf{e}}(s)\,ds + \tau\mathbf{m}(t) - \frac{\tau}{2}\int_t^{t+\tau}\boldsymbol{\mu}(s)\,ds \\ &= \frac{\tau}{2}\mathbf{v} + \frac{1}{2}\int_t^{t+\tau}(\dot{\mathbf{e}}(t+\tau) - \dot{\mathbf{e}}(s)) + (\dot{\mathbf{e}}(t) - \dot{\mathbf{e}}(s))\,ds \\ &\quad - \frac{1}{2}\int_t^{t+\tau}\Big(\int_t^{t+\tau}\dot{\mathbf{m}}(\eta) + \boldsymbol{\mu}(s)\,d\eta\Big)\,ds\,. \end{aligned}$$

Due to the inequality of Young and the absolute continuity of the integral (see, e.g., App. (20) in [24]),

$$\|\mathbf{v}\|_{\mathbf{L}^1(t,t+\tau;\mathbf{V})} \le \|\mathbf{v}\|_{\mathbf{L}^2(t,t+\tau;\mathbf{V})}\cdot\tau^{1/2} = o\big(\tau^{1/2}\big) \tag{26}$$

for every fixed $\mathbf{v} \in \mathbf{L}^2(t,t+\tau_0;\mathbf{V})$ and for all $\tau \le \tau_0$. We apply this result to $\dot{\mathbf{m}}, \boldsymbol{\mu} \in \mathbf{L}^2(t,t+\tau;\mathbf{H}^1)$, and the inequality of Korn allows us to prove the estimate

$$\begin{aligned} &\big\|\mathbf{D}\mathbf{\Psi}^{t+\tau,t}\bar{\mathbf{u}}(t)(\bar{\mathbf{e}}(t)) - \mathbf{e}(t+\tau) + \tau\mathbf{m}(t)\big\|_a \\ &\le \frac{\tau}{2}\big\|\mathbf{v}\big\|_a + \frac{1}{2}\int_t^{t+\tau}\big(\|\dot{\mathbf{e}}(t+\tau) - \dot{\mathbf{e}}(s)\|_{\mathbf{H}^1} + \|\dot{\mathbf{e}}(t) - \dot{\mathbf{e}}(s)\|_{\mathbf{H}^1}\big)\,ds \\ &\quad + \frac{\tau}{2}\big(\|\dot{\mathbf{m}}\|_{\mathbf{L}^1(t,t+\tau;\mathbf{H}^1)} + \|\boldsymbol{\mu}\|_{\mathbf{L}^1(t,t+\tau;\mathbf{H}^1)}\big) \\ &= \frac{\tau}{2}\big\|\mathbf{v}\big\|_a + \mathrm{TV}\big(\dot{\mathbf{e}},[t,t+\tau],\mathbf{H}^1\big)\cdot O(\tau) + o\big(\tau^{3/2}\big)\,. \end{aligned} \tag{27}$$

Since $\boldsymbol{\epsilon} = \dot{\mathbf{e}} - \mathbf{m} \in \mathbf{W}^{1,2}(t, t+\tau; \mathbf{H}^1, \mathbf{L}^2)$, integration by parts (see, e.g., Prop. 23.23 in [24]) and definition (22) yield

$$
\begin{aligned}
&\Big\|\dot{\mathbf{D}}\boldsymbol{\Psi}^{t+\tau,t}\bar{\mathbf{u}}(t)(\bar{\mathbf{e}}(t)) - \boldsymbol{\epsilon}(t+\tau) + \int_t^{t+\tau} \boldsymbol{\mu}(s)\,ds\Big\|_{\mathbf{L}^2}^2 = \|\mathbf{v}\|_{\mathbf{L}^2}^2 \\
&= \Big\langle \dot{\mathbf{D}}\boldsymbol{\Psi}^{t+\tau,t}\bar{\mathbf{u}}(t)(\bar{\mathbf{e}}(t)) - \boldsymbol{\epsilon}(t) - \int_t^{t+\tau} \dot{\boldsymbol{\epsilon}}(s) - \boldsymbol{\mu}(s)\,ds, \mathbf{v}\Big\rangle_{(\mathbf{H}^1)^*\times\mathbf{H}^1} \\
&= \Big\langle \dot{\mathbf{D}}\boldsymbol{\Psi}^{t+\tau,t}\bar{\mathbf{u}}(t)(\bar{\mathbf{e}}(t)) - \boldsymbol{\epsilon}(t) - \int_t^{t+\tau} \ddot{\mathbf{e}}(s) - \dot{\mathbf{m}}(s) - \boldsymbol{\mu}(s)\,ds, \mathbf{v}\Big\rangle_{(\mathbf{H}^1)^*\times\mathbf{H}^1} \\
&= \big\langle \dot{\mathbf{D}}\boldsymbol{\Psi}^{t+\tau,t}\bar{\mathbf{u}}(t)(\bar{\mathbf{e}}(t)) - \boldsymbol{\epsilon}(t) - \tau(\ddot{\mathbf{e}}(t) - \dot{\mathbf{m}}(t) - \boldsymbol{\mu}(t)), \mathbf{v}\big\rangle_{(\mathbf{H}^1)^*\times\mathbf{H}^1} \\
&\quad - \Big\langle \int_t^{t+\tau} \ddot{\mathbf{e}}(s) - \ddot{\mathbf{e}}(t)\,ds, \mathbf{v}\Big\rangle_{(\mathbf{H}^1)^*\times\mathbf{H}^1} - \Big\langle \int_t^{t+\tau} \Big(\int_t^s \ddot{\mathbf{m}}(\eta)\,d\eta\Big)\,ds, \mathbf{v}\Big\rangle_{(\mathbf{H}^1)^*\times\mathbf{H}^1} \\
&\le \big|\big\langle \dot{\mathbf{D}}\boldsymbol{\Psi}^{t+\tau,t}\bar{\mathbf{u}}(t)(\bar{\mathbf{e}}(t)) - \boldsymbol{\epsilon}(t) - \tau(\ddot{\mathbf{e}}(t) - \dot{\mathbf{m}}(t) - \boldsymbol{\mu}(t)), \mathbf{v}\big\rangle_{(\mathbf{H}^1)^*\times\mathbf{H}^1}\big| \\
&\quad + \Big(\int_t^{t+\tau} \|\ddot{\mathbf{e}}(s) - \ddot{\mathbf{e}}(t)\|_{(\mathbf{H}^1)^*}\,ds\Big)\|\mathbf{v}\|_{\mathbf{H}^1} + \tau\|\ddot{\mathbf{m}}\|_{\mathbf{L}^1(t,t+\tau;(\mathbf{H}^1)^*)}\|\mathbf{v}\|_{\mathbf{H}^1} \\
&= \big|\big\langle \dot{\mathbf{D}}\boldsymbol{\Psi}^{t+\tau,t}\bar{\mathbf{u}}(t)(\bar{\mathbf{e}}(t)) - \boldsymbol{\epsilon}(t) - \tau(\ddot{\mathbf{e}}(t) - \dot{\mathbf{m}}(t) - \boldsymbol{\mu}(t)), \mathbf{v}\big\rangle_{(\mathbf{H}^1)^*\times\mathbf{H}^1}\big| \\
&\quad + \mathrm{TV}\big(\ddot{\mathbf{e}}, [t, t+\tau], \mathbf{H}^1\big)\|\mathbf{v}\|_{\mathbf{H}^1}\cdot O(\tau) + \|\mathbf{v}\|_{\mathbf{H}^1}\cdot o\big(\tau^{3/2}\big)
\end{aligned}
$$

for the squared $\mathbf{L}^2$-norm. We insert the numerical scheme (7), the variational inequality (19), and definition (22) into the first term on the right-hand side of this estimate. Then, relation (10) and integration by parts lead to

$$
\begin{aligned}
&\big\langle \dot{\mathbf{D}}\boldsymbol{\Psi}^{t+\tau,t}\bar{\mathbf{u}}(t)(\bar{\mathbf{e}}(t)) - \boldsymbol{\epsilon}(t) - \tau(\ddot{\mathbf{e}}(t) - \dot{\mathbf{m}}(t) - \boldsymbol{\mu}(t)), \mathbf{v}\big\rangle_{(\mathbf{H}^1)^*\times\mathbf{H}^1} \\
&= -\frac{\tau^2}{4}\big\langle \mathbf{F}\big(\dot{\mathbf{D}}\boldsymbol{\Psi}^{t+\tau,t}\bar{\mathbf{u}}(t)(\bar{\mathbf{e}}(t)) + \boldsymbol{\epsilon}(t)\big), \mathbf{v}\big\rangle - \frac{\tau}{2}\big\langle \mathbf{G}\big(\dot{\mathbf{D}}\boldsymbol{\Psi}^{t+\tau,t}\bar{\mathbf{u}}(t)(\bar{\mathbf{e}}(t)) - \boldsymbol{\epsilon}(t)\big), \mathbf{v}\big\rangle \\
&\quad + \tau\big\langle \mathbf{F}_{\mathrm{con}}\big(\mathbf{D}\boldsymbol{\Psi}^{t+\tau,t}\bar{\mathbf{u}}(t)(\bar{\mathbf{e}}(t))\big) - \mathbf{F}_{\mathrm{con}}(\mathbf{e}(t)), \mathbf{v}\big\rangle_{(\mathbf{H}^1)^*\times\mathbf{H}^1} \\
&= -\frac{\tau^2}{4}\big\|\mathbf{v}\big\|_a^2 - \frac{\tau^2}{4}a\big(\boldsymbol{\epsilon}(t) + \boldsymbol{\epsilon}(t+\tau), \mathbf{v}\big) + \frac{\tau^2}{4}a\Big(\int_t^{t+\tau}\boldsymbol{\mu}(s)\,ds, \mathbf{v}\Big) \\
&\quad - \frac{\tau}{2}\big\|\mathbf{v}\big\|_b^2 - \frac{\tau}{2}b\big(\boldsymbol{\epsilon}(t+\tau) - \boldsymbol{\epsilon}(t), \mathbf{v}\big) + \frac{\tau}{2}b\Big(\int_t^{t+\tau}\boldsymbol{\mu}(s)\,ds, \mathbf{v}\Big) \\
&\quad + \tau\big\langle \mathbf{F}_{\mathrm{con}}\big(\mathbf{D}\boldsymbol{\Psi}^{t+\tau,t}\bar{\mathbf{u}}(t)(\bar{\mathbf{e}}(t))\big) - \mathbf{F}_{\mathrm{con}}(\mathbf{e}(t)), \mathbf{v}\big\rangle_{(\mathbf{H}^1)^*\times\mathbf{H}^1} \\
&= -\frac{\tau^2}{4}\big\|\mathbf{v}\big\|_a^2 - \frac{\tau^2}{4}a\big(\dot{\mathbf{e}}(t) + \dot{\mathbf{e}}(t+\tau), \mathbf{v}\big) + \frac{\tau^2}{4}a\Big(\mathbf{m}(t) + \mathbf{m}(t+\tau) + \int_t^{t+\tau}\boldsymbol{\mu}(s)\,ds, \mathbf{v}\Big) \\
&\quad - \frac{\tau}{2}\big\|\mathbf{v}\big\|_b^2 + \frac{\tau}{2}b\big(\dot{\mathbf{e}}(t+\tau) - \dot{\mathbf{e}}(t), \mathbf{v}\big) + \frac{\tau}{2}b\Big(\int_t^{t+\tau}\dot{\mathbf{m}}(s) + \boldsymbol{\mu}(s)\,ds, \mathbf{v}\Big) \\
&\quad + \tau\big\langle \mathbf{F}_{\mathrm{con}}\big(\mathbf{D}\boldsymbol{\Psi}^{t+\tau,t}\bar{\mathbf{u}}(t)(\bar{\mathbf{e}}(t))\big) - \mathbf{F}_{\mathrm{con}}(\mathbf{e}(t)), \mathbf{v}\big\rangle_{(\mathbf{H}^1)^*\times\mathbf{H}^1}\,.
\end{aligned}
$$

Due to the estimate (26) and the inequality of Korn, we find

$$\begin{aligned}
&\Big\|\dot{\mathbf{D}}\boldsymbol{\Psi}^{t+\tau,t}\bar{\mathbf{u}}(t)(\bar{\mathbf{e}}(t)) - \boldsymbol{\epsilon}(t+\tau) + \int_t^{t+\tau} \boldsymbol{\mu}(s)\,ds\Big\|_{\mathbf{L}^2}^2 + \frac{\tau}{2}\|\mathbf{v}\|_b^2 \\
&\le -\frac{\tau^2}{4}\|\mathbf{v}\|_a^2 + \frac{\tau^2}{4}\big(\|\dot{\mathbf{e}}(t)\|_{\mathbf{H}^1} + \|\dot{\mathbf{e}}(t+\tau)\|_{\mathbf{H}^1}\big)\|\mathbf{v}\|_{\mathbf{H}^1} \\
&\quad + \frac{\tau^2}{4}\big(\|\mathbf{m}(t)\|_{\mathbf{H}^1} + \|\mathbf{m}(t+\tau)\|_{\mathbf{H}^1} + \|\boldsymbol{\mu}\|_{\mathbf{L}^1(t,t+\tau;\mathbf{H}^1)}\big)\|\mathbf{v}\|_{\mathbf{H}^1} \\
&\quad + \frac{\tau}{2}\|\dot{\mathbf{e}}(t+\tau) - \dot{\mathbf{e}}(t)\|_{\mathbf{H}^1}\|\mathbf{v}\|_{\mathbf{H}^1} + \frac{\tau}{2}\big(\|\dot{\mathbf{m}}\|_{\mathbf{L}^1(t,t+\tau;\mathbf{H}^1)} + \|\boldsymbol{\mu}\|_{\mathbf{L}^1(t,t+\tau;\mathbf{H}^1)}\big)\|\mathbf{v}\|_{\mathbf{H}^1} \\
&\quad + \tau\big|\big\langle \mathbf{F}_{\text{con}}\big(\mathbf{D}\boldsymbol{\Psi}^{t+\tau,t}\bar{\mathbf{u}}(t)(\bar{\mathbf{e}}(t))\big) - \mathbf{F}_{\text{con}}(\mathbf{e}(t)), \mathbf{v}\big\rangle_{(\mathbf{H}^1)^*\times\mathbf{H}^1}\big| \\
&\quad + \big(\mathrm{TV}(\ddot{\mathbf{e}}, [t,t+\tau], \mathbf{H}^1) + o\big(\tau^{1/2}\big)\big)\|\mathbf{v}\|_{\mathbf{H}^1}\cdot O(\tau) \\
&= -\frac{\tau^2}{4}\|\mathbf{v}\|_a^2 + \tau\big|\big\langle \mathbf{F}_{\text{con}}\big(\mathbf{D}\boldsymbol{\Psi}^{t+\tau,t}\bar{\mathbf{u}}(t)(\bar{\mathbf{e}}(t))\big) - \mathbf{F}_{\text{con}}(\mathbf{e}(t)), \mathbf{v}\big\rangle_{(\mathbf{H}^1)^*\times\mathbf{H}^1}\big| \\
&\quad + \big(\mathrm{TV}\big(\dot{\mathbf{e}}, [t,t+\tau], \mathbf{H}^1\big) + \mathrm{TV}\big(\ddot{\mathbf{e}}, [t,t+\tau], \mathbf{H}^1\big) + o\big(\tau^{1/2}\big)\big)\|\mathbf{v}\|_{\mathbf{H}^1}\cdot O(\tau)\,.
\end{aligned}$$

Adding the square of (27), the inequality of Young leads to

$$\begin{aligned}
&\frac{1}{2}\Big\|\dot{\mathbf{D}}\boldsymbol{\Psi}^{t+\tau,t}\bar{\mathbf{u}}(t)(\bar{\mathbf{e}}(t)) - \boldsymbol{\epsilon}(t+\tau) + \int_t^{t+\tau} \boldsymbol{\mu}(s)\,ds\Big\|_{\mathbf{L}^2}^2 \\
&+ \frac{1}{2}\big\|\mathbf{D}\boldsymbol{\Psi}^{t+\tau,t}\bar{\mathbf{u}}(t)(\bar{\mathbf{e}}(t)) - \mathbf{e}(t+\tau) + \tau\mathbf{m}(t)\big\|_a^2 + \frac{\tau}{4}\|\mathbf{v}\|_b^2 \\
&= \frac{\tau}{2}\big|\big\langle \mathbf{F}_{\text{con}}\big(\mathbf{D}\boldsymbol{\Psi}^{t+\tau,t}\bar{\mathbf{u}}(t)(\bar{\mathbf{e}}(t))\big) - \mathbf{F}_{\text{con}}(\mathbf{e}(t)), \mathbf{v}\big\rangle_{(\mathbf{H}^1)^*\times\mathbf{H}^1}\big| \\
&\quad + \big(R(\mathbf{e}, [t,t+\tau])\cdot O(\tau) + o\big(\tau^{3/2}\big)\big)^2 + \big(R(\mathbf{e}, [t,t+\tau]) + o\big(\tau^{1/2}\big)\big)\|\mathbf{v}\|_{\mathbf{H}^1}\cdot O(\tau)\,.
\end{aligned}$$

This is an estimate of the type

$$x^2 + \frac{\tau}{4}\|\mathbf{v}\|_b^2 \le a^2 + b\|\mathbf{v}\|_{\mathbf{H}^1}\cdot\tau$$

with $a, b > 0$, and $x^2\cdot\tau^{2p}$ is the right-hand side of (25). The inequality of Korn yields

$$\|\mathbf{v}\|_{\mathbf{H}^1} \le \frac{1}{c_K}\big(\|\mathbf{v}\|_{\mathbf{L}^2}^2 + \|\mathbf{v}\|_b^2\big)^{1/2} \le \frac{2}{c_K}\Big(x^2 + \frac{\tau}{4}\|\mathbf{v}\|_b^2\Big)^{1/2}\cdot\tau^{-1/2}$$

for τ sufficiently small. Hence,

$$x^2 + \frac{\tau}{4}\|\mathbf{v}\|_b^2 \le a^2 + \frac{2b}{c_K}\Big(x^2 + \frac{\tau}{4}\|\mathbf{v}\|_b^2\Big)^{1/2}\cdot\tau^{1/2}$$

and by means of the binomial formula, this is equivalent to

$$\bigg(\Big(x^2 + \frac{\tau}{4}\|\mathbf{v}\|_b^2\Big)^{1/2} - \frac{b}{c_K}\cdot\tau^{1/2}\bigg)^2 \le a^2 + \frac{b^2}{c_K^2}\cdot\tau\,.$$

Finally,

$$\Big(x^2 + \frac{\tau}{4}\|\mathbf{v}\|_b^2\Big)^{1/2} \le a + b\cdot O\big(\tau^{1/2}\big)$$

and (25) gives the result of the lemma. $\square$

With these rather lengthy preparations, we are now ready to prove the central theorem of this paper.

Theorem 3.9. *Let Assumptions* 3.4 *and* 3.6 *hold. Then, the consistency error in terms of the discrete evolution* $\bar{\mathbf{\Psi}}_* = (\mathbf{\Psi}_*, \dot{\mathbf{\Psi}}_*)$ *satisfies*

$$\begin{aligned}
&\big\| \bar{\mathbf{\Psi}}_*^{t+\tau,t} \bar{\mathbf{u}}(t) - \bar{\mathbf{\Phi}}^{t+\tau,t} \bar{\mathbf{u}}(t) - (\bar{\mathbf{r}}(t,\tau) + \bar{\mathbf{p}}(t,\tau)) \cdot \tau^p \big\|_E \\
&= \Big(\big\| \mathbf{F}_{\mathrm{con}}\big(\mathbf{D\Psi}^{t+\tau,t}\bar{\mathbf{u}}(t)(\bar{\mathbf{e}}(t))\big) - \mathbf{F}_{\mathrm{con}}(\mathbf{e}(t)) \big\|_{(H^1)^*} + R(\mathbf{e},[t,t+\tau]) \Big) \cdot O\big(\tau^{p+1/2}\big) \\
&\quad + o\big(\tau^{p+1}\big)
\end{aligned} \tag{28}$$

with $R(\mathbf{e},[t,t+\tau])$ *defined in* (13).

Proof. With $\mathbf{v} := \dot{\mathbf{D}}\mathbf{\Psi}^{t+\tau,t}\bar{\mathbf{u}}(t)(\bar{\mathbf{e}}(t)) - \boldsymbol{\epsilon}(t+\tau) + \int_t^{t+\tau} \boldsymbol{\mu}(s)\,ds$, Lemma 3.7 yields

$$\begin{aligned}
&\Big(\big\| \bar{\mathbf{\Psi}}_*^{t+\tau,t} \bar{\mathbf{u}}(t) - \bar{\mathbf{\Phi}}^{t+\tau,t} \bar{\mathbf{u}}(t) - (\bar{\mathbf{r}}(t,\tau) + \bar{\mathbf{p}}(t,\tau)) \cdot \tau^p \big\|_E^2 + \frac{\tau}{4} \big\| \mathbf{v} \big\|_b^2 \cdot \tau^{2p} \Big)^{1/2} \\
&\le \Big(\frac{1}{2} \big\| \mathbf{F}_{\mathrm{con}}\big(\mathbf{D\Psi}^{t+\tau,t}\bar{\mathbf{u}}(t)(\bar{\mathbf{e}}(t))\big) - \mathbf{F}_{\mathrm{con}}(\mathbf{e}(t)) \big\|_{(\mathbf{H}^1)^*} \Big)^{1/2} \|\mathbf{v}\|_{\mathbf{H}^1}^{1/2} \cdot \tau^{p+1/2} \\
&\quad + R(\mathbf{e},[t,t+\tau]) \cdot O\big(\tau^{p+1/2}\big) + o\big(\tau^{p+1}\big) \,.
\end{aligned}$$

This is an estimate of the form

$$\Big(x^2 + \frac{\tau}{4} \big\| \mathbf{v} \big\|_b^2 \cdot \tau^{2p} \Big)^{1/2} \le a + b^{1/2} \|\mathbf{v}\|_{\mathbf{H}^1}^{1/2} \cdot \tau^{p+1/2}$$

with $a, b, x > 0$. The inequality of Young leads to

$$\Big(x^2 + \frac{\tau}{4} \big\| \mathbf{v} \big\|_b^2 \cdot \tau^{2p} \Big)^{1/2} \le a + \alpha b \cdot \tau^{p+1/2} + \frac{1}{\alpha} \|\mathbf{v}\|_{\mathbf{H}^1} \cdot \tau^{p+1/2}$$

with $\alpha > 0$, and due to the inequality of Korn

$$\|\mathbf{v}\|_{\mathbf{H}^1} \cdot \tau^{p+1/2} \le \frac{1}{c_K} \big(\|\mathbf{v}\|_{\mathbf{L}^2}^2 + \|\mathbf{v}\|_b^2 \big)^{1/2} \cdot \tau^{p+1/2} \le \frac{2}{c_K} \Big(x^2 + \frac{\tau}{4} \big\| \mathbf{v} \big\|_b^2 \cdot \tau^{2p} \Big)^{1/2}$$

for τ sufficiently small. Choosing $\alpha = 4/c_K$, we can reformulate the estimate above as

$$\frac{1}{2} \Big(x^2 + \frac{\tau}{4} \big\| \mathbf{v} \big\|_b^2 \cdot \tau^{2p} \Big)^{1/2} \le a + \frac{4b}{c_K} \cdot \tau^{p+1/2}$$

such that

$$x = O\big(a + b \cdot \tau^{p+1/2} \big) \,.$$

□

3.3 Discussion of consistency order

Our purpose in the previous section was to construct the discrete evolution operator $(\mathbf{\Psi}_*, \dot{\mathbf{\Psi}}_*)$ such that the resulting scheme is of higher consistency order in energy norm than CSN, compare condition (16). In order to analyze the actual order of the scheme, we want to discuss the result of Theorem 3.9 in detail.

First of all, the error estimate (28) contains the remainder term $\bar{\mathbf{r}}(t,\tau)$ of Assumption 3.4 on the consistency error of CSN which strongly depends on the choice of the order p. The consistency result 2.3 in energy norm does not give any information about the local behavior of the error in space. In order to gain some insight into this problem, we present a numerical study concerning the spatial distribution of the consistency error of CSN.

Numerical Experiment. As an illustrative test problem, we select a Hertzian contact in 2D. At initial time $t = 0$, we have a half circle with radius $r = 0.15$ and

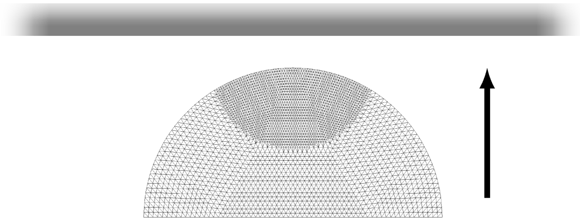

Figure 1: Test problem.

midpoint on the y–axis. The semicircle has an initial distance 0.05 to a plate on the x–axis and is moving up with vertical speed $\dot{\mathbf{u}}(0) = (0, 1)$. The possible contact boundary consists of a sixth circle located at the top. The remaining part of the boundary is traction-free and no volume forces occur. The underlying triangulation results from 5 refinement steps of a coarse grid triangulation with 3 vertices. We refine five times further within a circle of radius 0.08 around the top of the semicircle. The computational meshes are shown in Figure 1, and the elastic and viscous material parameters can be found in Table 1.

parameter	value
Young's modulus	10
Poisson ratio	0.4
shear viscosity	10
bulk viscosity	10

Table 1: Material specifications.

In order to get an approximation of the exact solution of the variational problem, we perform CSN with an extremely high timestep resolution. The difference between this fine reference solution and one large step of CSN acts as an indicator for the consistency error of the scheme.

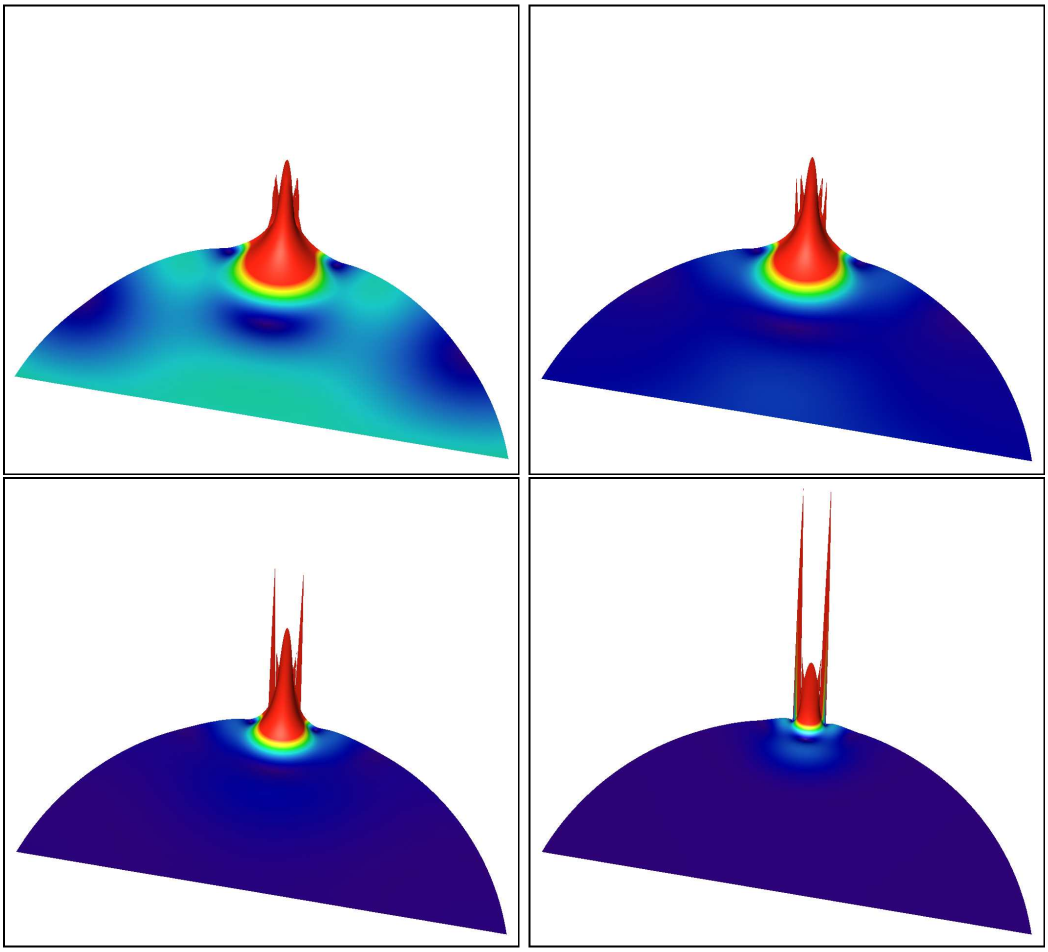

Figure 2: Spatial distribution of the estimated temporal consistency error of CSN for $\tau \to 0$ (4 snapshots).

Figure 2 shows the time evolution of the estimated consistency error of CSN as the timestep τ tends to zero. We observe that the domain where the error has a significant value shrinks for decreasing timesteps. For small τ, the error is concentrated near those parts of the contact boundary where the active set changes. Moreover, we find that the error consists of two different parts, a regular one in the interior of the domain and a second one at the changing active contact boundary. This effect corresponds to our theoretical analysis of the consistency error as discussed in Remark 3.8 and will become important for our timestep control in Section 4.

The observations above lead us to the following conjecture on the local behavior of the consistency error. Due to the viscous material behavior, the irregularity of the problem from the changing active contact boundaries is smoothened in the interior of the domain. If we pick a suitable subdomain $\tilde{\Omega}$ of Ω with positive minimal distance to the contact boundaries, then we expect to find the maximal order of consistency $p = 2$ on $\tilde{\Omega}$, eventually for small τ. However, the range of τ for which the asymptotic behavior becomes visible most likely depends on the choice of $\tilde{\Omega}$. We may now exhaust Ω by a sequence of sets $\tilde{\Omega}_k \subset \tilde{\Omega}_{k+1} \subset \dots$ to find maximal order of consistency on each of these sets, but a lower total order of consistency on the whole domain Ω.

The local behavior of the consistency error (and the sensitivity) of CSN is reflected in the assumption

$$\|\bar{\mathbf{r}}(t,\tau) + \bar{\mathbf{p}}(t,\tau)\|_{E(\tilde{\Omega})} \cdot \tau^2 = o\big(\tau^3\big)$$

where we denote the physical energy norm w.r.t. the subdomain $\tilde{\Omega}$ by $\|\cdot\|_{E(\tilde{\Omega})}$. Applying the lower triangle inequality on the result of Theorem 3.9 with $p = 2$, we find the consistency error estimate

$$\begin{aligned}
&\big\|\bar{\mathbf{\Psi}}_*^{t+\tau,t}\bar{\mathbf{u}}(t) - \bar{\mathbf{\Phi}}^{t+\tau,t}\bar{\mathbf{u}}(t)\big\|_{E(\tilde{\Omega})} \\
&\le \Big(\big\|\mathbf{F}_{\text{con}}\big(\mathbf{D}\mathbf{\Psi}^{t+\tau,t}\bar{\mathbf{u}}(t)(\bar{\mathbf{e}}(t))\big) - \mathbf{F}_{\text{con}}(\mathbf{e}(t))\big\|_{(\mathbf{H}^1(\Omega))^*} + R(\mathbf{e},[t,t+\tau])\Big) \cdot O\big(\tau^{5/2}\big) \\
&\quad + \|(\bar{\mathbf{r}}(t,\tau) + \bar{\mathbf{p}}(t,\tau))\|_{E(\tilde{\Omega})} \cdot \tau^2 + o\big(\tau^3\big) \\
&= \Big(\big\|\mathbf{F}_{\text{con}}\big(\mathbf{D}\mathbf{\Psi}^{t+\tau,t}\bar{\mathbf{u}}(t)(\bar{\mathbf{e}}(t))\big) - \mathbf{F}_{\text{con}}(\mathbf{e}(t))\big\|_{(\mathbf{H}^1(\Omega))^*} + R(\mathbf{e},[t,t+\tau])\Big) \cdot O\big(\tau^{5/2}\big) \\
&\quad + o\big(\tau^3\big)
\end{aligned}$$

on $\tilde{\Omega}$. In Remark 3.8, we have discussed that the difference of the contact forces $\mathbf{F}_{\text{con}}\big(\mathbf{D}\mathbf{\Psi}^{t+\tau,t}\bar{\mathbf{u}}(t)(\bar{\mathbf{e}}(t))\big)$ and $\mathbf{F}_{\text{con}}(\mathbf{e}(t))$ only act on a small part of the possible contact boundaries which is expected to tend to zero for most times t as $\tau \to 0$. However, for ease of presentation, we have neglected this behavior by applying an $(\mathbf{H}^1(\Omega))^*$-norm estimate. This norm depends on the behavior of the differences $\mathbf{D}\mathbf{\Psi}^{t+\tau,t}\bar{\mathbf{u}}(t)(\bar{\mathbf{e}}(t)) - \mathbf{e}(t)$ and $\dot{\mathbf{D}}\mathbf{\Psi}^{t+\tau,t}\bar{\mathbf{u}}(t)(\bar{\mathbf{e}}(t)) - \boldsymbol{\epsilon}(t)$ which tend to zero in $\mathbf{H}^1$, resp. in $\mathbf{L}^2$. For most times t, we may even expect an $\mathbf{H}^1$-convergence to zero of order τ, and the assumption

$$\big\|\mathbf{F}_{\text{con}}\big(\mathbf{D}\mathbf{\Psi}^{t+\tau,t}\bar{\mathbf{u}}(t)(\bar{\mathbf{e}}(t))\big) - \mathbf{F}_{\text{con}}(\mathbf{e}(t))\big\|_{(\mathbf{H}^1(\Omega))^*} = O(\tau)$$

is reasonable. The quantity $R(\mathbf{e},[t,t+\tau])$ corresponds to the right-hand side of the consistency result 2.3 which contains $R(\mathbf{u},[t,t+\tau])$ in turn. Since $\bar{\mathbf{e}}$ and $\bar{\mathbf{u}}$ are defined via variational inequalities with coinciding active contact boundaries, we expect that $R(\mathbf{e},[t,t+\tau])$ originates from a quantity which has a similar local behavior as the consistency error of CSN. However, since $R(\mathbf{e},[t,t+\tau])$ refers to the whole domain Ω, we restrict our considerations to

$$R(\mathbf{e},[t,t+\tau]) = O(\tau)$$

which again is a reasonable assumption, at least for most times t. Then, we find

$$\big\|\bar{\mathbf{\Psi}}_*^{t+\tau,t}\bar{\mathbf{u}}(t) - \bar{\mathbf{\Phi}}^{t+\tau,t}\bar{\mathbf{u}}(t)\big\|_{E(\tilde{\Omega})} = o\big(\tau^3\big)\,, \tag{29}$$

and the scheme $(\boldsymbol{\Psi}_*, \dot{\boldsymbol{\Psi}}_*)$ is of higher consistency order on $\tilde{\Omega}$ than CSN. In summary, we expect an asymptotic error expansion of CSN with order $p = 2$ which is visible on a subdomain in the interior.

4 Timestep Control

In this section, our aim is to develop a strategy for choosing the size of timesteps for the contact–stabilized Newmark method adaptively. This variant of CSN will be called ContacX further on.

Ideally, an adaptive timestep control guarantees that the global discretization error of the approximation is below a prescribed tolerance. However, global errors are difficult to control since they consist of the actual consistency error as well as the propagation of all errors that arise during time integration. We follow the standard approach, and we intend to control the actual consistency error in the reduced physical energy norm such that

$$\left\| \bar{\boldsymbol{\Psi}} - \bar{\boldsymbol{\Phi}} \right\|_E \leq \mathrm{TOL} \tag{30}$$

where TOL is a *local tolerance* defined by the user. The idea behind is that smaller consistency errors lead to a decrease of the global error. Since we cannot determine this error exactly, we need a computable estimate

$$\left[\left\| \bar{\boldsymbol{\Psi}} - \bar{\boldsymbol{\Phi}} \right\|_E \right] \approx \left\| \bar{\boldsymbol{\Psi}} - \bar{\boldsymbol{\Phi}} \right\|_E ,$$

and we look for the implementable condition

$$\left[\left\| \bar{\boldsymbol{\Psi}} - \bar{\boldsymbol{\Phi}} \right\|_E \right] \leq \mathrm{TOL} .$$

The construction of a problem-adapted *error estimator* is the main challenge in the establishment of an adaptive timestep control. Let $\bar{\hat{\boldsymbol{\Psi}}} := \left(\hat{\boldsymbol{\Psi}}, \dot{\hat{\boldsymbol{\Psi}}} \right)$ be a second discrete evolution which is of higher accuracy than CSN for sufficiently small timesteps. Then, the difference between the two numerical solutions is an error estimator, and we set

$$\left[\left\| \bar{\boldsymbol{\Psi}} - \bar{\boldsymbol{\Phi}} \right\|_E \right] := \left\| \bar{\boldsymbol{\Psi}} - \bar{\hat{\boldsymbol{\Psi}}} \right\|_E .$$

If the more accurate time integration scheme is even of higher consistency order than CSN, then the error estimator is asymptotically exact (for more details see, e.g., [5]).

In order to develop a comparative scheme of higher order, we intend to employ extrapolation techniques which require an asymptotic error expansion of CSN. As we have seen in the foregoing Section 3, the classical theory can not directly be applied to dynamical contact problems due to the missing regularity at time-dependent contact boundaries. In order to ensure a reliable timestep control, we have to adapt the classical error estimator and timestep selection in the presence of contact.

4.1 Error estimator in the absence of contact

In the absence of contact, CSN has pointwise optimal consistency order $p = 2$ both in displacements and velocities. Furthermore, the consistency error has a pointwise Taylor expansion due to the linearity of the problem. Hence, the results of Section 3 yield the existence of an asymptotic error expansion of the Newmark method.

$$
\begin{array}{rcccc}
\bar{\boldsymbol{u}}_{\tau} & = & \bar{\boldsymbol{u}}_{11} & \searrow & \\
\bar{\boldsymbol{u}}_{\frac{\tau}{2}} & = & \bar{\boldsymbol{u}}_{21} & \longrightarrow & \bar{\boldsymbol{u}}_{22}
\end{array}
$$

Figure 3: Extrapolation table in the absence of contact, compare Fig. 4.

In order to construct a scheme of higher order, we follow a one-step extrapolation method, see Figure 3, and we compute a second numerical solution with half timestep $\tau/2$. Then, we consider the asymptotic error expansions

$$
\begin{aligned}
\bar{\mathbf{u}}_{11}(t+\tau) &= \bar{\mathbf{u}}(t+\tau) + \bar{\mathbf{e}}(t+\tau)\tau^2 + o(\tau^3) \\
\bar{\mathbf{u}}_{21}(t+\tau) &= \bar{\mathbf{u}}(t+\tau) + \bar{\mathbf{e}}(t+\tau)\Big(\frac{\tau}{2}\Big)^2 + o(\tau^3)
\end{aligned} \tag{31}
$$

of CSN. The extrapolated method

$$
\bar{\mathbf{u}}_{22}(t+\tau) := \frac{1}{1-2^2}\big(\bar{\mathbf{u}}_{11}(t+\tau) - 2^2\bar{\mathbf{u}}_{21}(t+\tau)\big) \tag{32}
$$

is of higher consistency order in energy norm than CSN since

$$
\begin{aligned}
&\|\bar{\mathbf{u}}_{22}(t+\tau) - \bar{\mathbf{u}}(t+\tau)\|_E \\
&\le \frac{1}{2^2-1}\big\|\bar{\mathbf{u}}_{11}(t+\tau) - \bar{\mathbf{u}}(t+\tau) - \bar{\mathbf{e}}(t+\tau)\tau^2\big\|_E \\
&\quad + \frac{2^2}{2^2-1}\Big\|\bar{\mathbf{u}}_{21}(t+\tau) - \bar{\mathbf{u}}(t+\tau) - \bar{\mathbf{e}}(t+\tau)\Big(\frac{\tau}{2}\Big)^2\Big\|_E \\
&= o(\tau^3)\,.
\end{aligned}
$$

We choose the *subdiagonal* error estimator

$$
\big[\|\bar{\mathbf{u}}_{21}(t+\tau) - \bar{\mathbf{u}}(t+\tau)\|_E\big] := \|\bar{\mathbf{u}}_{21}(t+\tau) - \bar{\mathbf{u}}_{22}(t+\tau)\|_E \tag{33}
$$

since we want to continue the computation with the higher order solution $\bar{\mathbf{u}}_{21}(t+\tau)$. The extrapolated solution $\bar{\mathbf{u}}_{22}(t+\tau)$ is not practical due to the missing energy dissipativity of the scheme. The choice of a subdiagonal error estimator avoids that condition (30) is over satisfied (see, e.g., [5]).

4.2 Error estimator in the presence of contact

If we find active contact boundaries in a time interval, we have to take into account the discussion on the existence of an asymptotic error expansion of CSN in Section 3.

Due to our theoretical insight in Remark 3.8 and our numerical observations in Section 3.3, the consistency error seems to consist of two different parts. The first one acts on points in the interior of the domain and is assumed to be of optimal order $p = 2$. The second one becomes extremely large at points near changing active contact boundaries. The extrapolated solution (32) is of higher consistency order than CSN only at points which have already reached the asymptotic phase $p = 2$. Hence, the classical error estimator (33) is only applicable on a subdomain. If this subdomain grows as the timestep tends to zero, the estimator becomes more and more accurate for small τ. However, the classical approach underestimates the remainder terms in the asymptotic error expansion near the critical changing contact boundaries.

In order to control the additional contribution to the consistency error in the presence of contact, we add a quantity $\bar{\mathbf{X}} := (\mathbf{X}, \dot{\mathbf{X}})$ to our model for the approximation error. The term including $\bar{\mathbf{X}}$ may be of worst possible order $p = 0.5$ as shown by our consistency result 2.3 up to sets of measure zero. The quantity should have a significant value at points near those parts of the active contact boundaries which vary within the timestep. In the limit $\tau \to 0$, the domain where the quantity vanishes should increase.

Again, we compute two numerical solutions with timesteps τ and $\tau/2$, and we make the ansatz

$$\begin{aligned} \bar{\mathbf{u}}_{11}(t+\tau) &\approx \bar{\mathbf{u}}(t+\tau) + \bar{\mathbf{e}}(t+\tau)\tau^2 + \bar{\mathbf{X}}(t+\tau)\tau^{1/2} \\ \bar{\mathbf{u}}_{21}(t+\tau) &\approx \bar{\mathbf{u}}(t+\tau) + \bar{\mathbf{e}}(t+\tau)\Big(\frac{\tau}{2}\Big)^2 + \bar{\mathbf{X}}(t+\tau)\Big(\frac{\tau}{2}\Big)^{1/2} \end{aligned} \tag{34}$$

for the approximation error. Within this model, the extrapolated solution $\bar{\mathbf{u}}_{22}(t+\tau)$ from (32) satisfies

$$\bar{\mathbf{u}}_{22}(t+\tau) \approx \bar{\mathbf{u}}(t+\tau) + \frac{1-2^{2-1/2}}{1-2^2}\bar{\mathbf{X}}(t+\tau)\tau^{1/2}\,.$$

In order to handle the low order term in this formula, we extend the extrapolation table by a third solution with timestep $\tau/3$, see Figure 4.

$$\begin{tikzcd}
\bar{\boldsymbol{u}}_{\tau} = \bar{\boldsymbol{u}}_{11} \arrow[dr] & \\
\bar{\boldsymbol{u}}_{\frac{\tau}{2}} = \bar{\boldsymbol{u}}_{21} \arrow[r] \arrow[dr] & \bar{\boldsymbol{u}}_{22} \\
\bar{\boldsymbol{u}}_{\frac{\tau}{3}} = \bar{\boldsymbol{u}}_{31} \arrow[r] & \bar{\boldsymbol{u}}_{32}
\end{tikzcd}$$

Figure 4: Extrapolation table in the presence of contact, compare Fig. 3.

This approximation satisfies

$$\bar{\mathbf{u}}_{31}(t+\tau) \approx \bar{\mathbf{u}}(t+\tau) + \bar{\mathbf{e}}(t+\tau)\Big(\frac{\tau}{3}\Big)^2 + \bar{\mathbf{X}}(t+\tau)\Big(\frac{\tau}{3}\Big)^{1/2}, \tag{35}$$

and the extrapolated solution

$$\bar{\mathbf{u}}_{32}(t+\tau) := \frac{1}{2^2-3^2}\big(2^2\bar{\mathbf{u}}_{21}(t+\tau) - 3^2\bar{\mathbf{u}}_{31}(t+\tau)\big) \tag{36}$$

yields

$$\bar{\mathbf{u}}_{32}(t+\tau) \approx \bar{\mathbf{u}}(t+\tau) + \frac{2^{2-1/2}-3^{2-1/2}}{2^2-3^2}\bar{\mathbf{X}}(t+\tau)\tau^{1/2}\,.$$

In a next step, we combine both extrapolation schemes via

$$\bar{\hat{\mathbf{u}}}(t+\tau) := \frac{1}{\alpha-\beta}(\alpha\bar{\mathbf{u}}_{22}(t+\tau) - \beta\bar{\mathbf{u}}_{32}(t+\tau)) \tag{37}$$

with

$$\alpha = \frac{2^{2-1/2}-3^{2-1/2}}{2^2-3^2}\,, \quad \beta = \frac{1-2^{2-1/2}}{1-2^2} \tag{38}$$

such that

$$\bar{\hat{\mathbf{u}}}(t+\tau) \approx \bar{\mathbf{u}}(t+\tau)\,.$$

As before, we proceed with the finest solution $\bar{\mathbf{u}}_{31}(t+\tau)$. Hence, we take the subdiagonal error estimator

$$\big[\|\bar{\mathbf{u}}_{31}(t+\tau) - \bar{\mathbf{u}}(t+\tau)\|_E\big] := \|\bar{\mathbf{u}}_{31}(t+\tau) - \bar{\hat{\mathbf{u}}}(t+\tau)\|_E\,. \tag{39}$$

Due to

$$\begin{aligned}&\big[\|\bar{\mathbf{u}}_{31}(t+\tau) - \bar{\mathbf{u}}(t+\tau)\|_E\big] \\ &\approx \Big\|\bar{\mathbf{u}}_{31}(t+\tau) - \bar{\mathbf{u}}_{32}(t+\tau) - \frac{2^{2-1/2}-3^{2-1/2}}{2^2-3^2}\bar{\mathbf{X}}(t+\tau)\tau^{1/2}\Big\|_E\,,\end{aligned}$$

the constructed error estimator consists of two parts. The first one corresponds to the classical estimator (33) with timestep $\tau/3$. The second one is relative to the quantity $\bar{\mathbf{X}}(t+\tau)$ in the asymptotic error expansion and mainly acts near the changing contact boundaries. Hence, the error estimator takes into account the special structure of the consistency error of CSN as it has been shown by our theoretical investigations in Remark 3.8 and our numerical experiment in Section 3.3.

4.3 Combined timestep strategy

The construction of an adaptive timestep control requires a suggestion for the new timestep from the actual information. Usually, this timestep is given by the optimal timestep τ^* for the actual step which is characterized by

$$\|\bar{\mathbf{u}}_{21}(t+\tau^*) - \bar{\mathbf{u}}(t+\tau^*)\|_E \approx \rho\cdot\mathrm{TOL}\,, \tag{40}$$

respectively

$$\|\bar{\mathbf{u}}_{31}(t+\tau^*) - \bar{\mathbf{u}}(t+\tau^*)\|_E \approx \rho\cdot\mathrm{TOL} \tag{41}$$

with a *safety factor* $\rho < 1$.

No contact. In the absence of contact, we assume that $\bar{\mathbf{e}}(t+\tau) \approx \dot{\bar{\mathbf{e}}}(t)\cdot\tau$. Inserting this approximation into the asymptotic error expansion (31) of CSN yield

$$\bar{\mathbf{u}}_{21}(t+\tau) - \bar{\mathbf{u}}(t+\tau) \approx \dot{\bar{\mathbf{e}}}(t)\tau \cdot \left(\frac{\tau}{2}\right)^2$$

for all τ up to terms of higher order. This leads to

$$\bar{\mathbf{u}}_{21}(t+\tau^*) - \bar{\mathbf{u}}(t+\tau^*) \approx (\bar{\mathbf{u}}_{21}(t+\tau) - \bar{\mathbf{u}}(t+\tau)) \cdot \left(\frac{\tau^*}{\tau}\right)^3 .$$

Taking the energy norm of this approximation and inserting condition (40), we can predict the optimal timestep τ^* by the classical timestep formula

$$\tau^* = \sqrt[3]{\frac{\rho \cdot \mathrm{TOL}}{\|\bar{\mathbf{u}}_{21}(t+\tau) - \bar{\mathbf{u}}_{22}(t+\tau)\|_E}} \cdot \tau . \tag{42}$$

Contact. In the presence of contact, our ansatz (35) for the discretization error of CSN and the assumption $\bar{\mathbf{e}}(t+\tau) \approx \dot{\bar{\mathbf{e}}}(t)\cdot\tau$ yield

$$\bar{\mathbf{u}}_{31}(t+\tau^*) - \bar{\mathbf{u}}(t+\tau^*) \approx \bar{\mathbf{e}}(t+\tau)\left(\frac{\tau}{3}\right)^2\left(\frac{\tau^*}{\tau}\right)^3 + \bar{\mathbf{X}}(t+\tau^*)\left(\frac{\tau^*}{3}\right)^{1/2} .$$

We have to make sure that $\tau^* < \tau$ if $\|\bar{\mathbf{u}}_{31}(t+\tau) - \hat{\bar{\mathbf{u}}}(t+\tau)\|_E > \rho\cdot\mathrm{TOL}$. For this purpose, we use the relation

$$\bar{\mathbf{u}}_{31}(t+\tau) - \hat{\bar{\mathbf{u}}}(t+\tau) \approx \bar{\mathbf{e}}(t+\tau)\left(\frac{\tau}{3}\right)^2 + \bar{\mathbf{X}}(t+\tau)\left(\frac{\tau}{3}\right)^{1/2}$$

and the triangle inequality to find that

$$\begin{aligned} &\left\|\bar{\mathbf{u}}_{31}(t+\tau^*) - \bar{\mathbf{u}}(t+\tau^*)\right\|_E \\ &\gtrsim \left\|\bar{\mathbf{u}}_{31}(t+\tau) - \hat{\bar{\mathbf{u}}}(t+\tau)\right\|_E \cdot \left(\frac{\tau^*}{\tau}\right)^3 \\ &\quad + \left|\left\|\bar{\mathbf{X}}(t+\tau^*)\right\|_E\left(\frac{\tau^*}{3}\right)^{1/2} - \left\|\bar{\mathbf{X}}(t+\tau)\right\|_E\left(\frac{\tau}{3}\right)^{1/2}\left(\frac{\tau^*}{\tau}\right)^3\right| . \end{aligned}$$

Due to condition (41), we look for

$$\begin{aligned} \rho\cdot\mathrm{TOL} = &\left\|\bar{\mathbf{u}}_{31}(t+\tau) - \hat{\bar{\mathbf{u}}}(t+\tau)\right\|_E \cdot \left(\frac{\tau^*}{\tau}\right)^3 \\ &+ \left|\left\|\bar{\mathbf{X}}(t+\tau^*)\right\|_E\left(\frac{\tau^*}{3}\right)^{1/2} - \left\|\bar{\mathbf{X}}(t+\tau)\right\|_E\left(\frac{\tau}{3}\right)^{1/2}\left(\frac{\tau^*}{\tau}\right)^3\right| . \end{aligned} \tag{43}$$

The quantity $\bar{\mathbf{X}}(t+\tau^*)$ does not necessarily tend to zero as $\tau \to 0$. Thus, we make the careful assumption $\|\bar{\mathbf{X}}(t+\tau^*)\|_E = \|\bar{\mathbf{X}}(t+\tau)\|_E$, and the optimal timestep τ^* is determined by

$$\begin{aligned} &\left\|\bar{\mathbf{u}}_{31}(t+\tau) - \hat{\bar{\mathbf{u}}}(t+\tau)\right\|_E\left(\frac{\tau^*}{\tau}\right)^3 + \left\|\bar{\mathbf{X}}(t+\tau)\right\|_E\left(\frac{\tau}{3}\right)^{1/2}\left|\left(\frac{\tau^*}{\tau}\right)^{1/2} - \left(\frac{\tau^*}{\tau}\right)^3\right| \\ &= \rho\cdot\mathrm{TOL} . \end{aligned} \tag{44}$$

Taking suitable differences of the approximations (34) and (35), the unknown quantity $\bar{\mathbf{X}}(t+\tau)$ may be estimated via

$$\begin{aligned}&\bar{\mathbf{X}}(t+\tau)\frac{\delta-\gamma}{\delta}\frac{1-\frac{1}{2^{1/2}}}{1-\frac{1}{2^2}}\tau^{1/2}\\&\approx 2^2(\bar{\mathbf{u}}_{21}(t+\tau)-\bar{\mathbf{u}}_{22}(t+\tau))-3^2(\bar{\mathbf{u}}_{31}(t+\tau)-\bar{\mathbf{u}}_{32}(t+\tau))\end{aligned}$$

with

$$\gamma=\Big(\frac{1}{2^{1/2}}-\frac{1}{3^{1/2}}\Big)\Big(1-\frac{1}{2^2}\Big),\quad \delta=\Big(\frac{1}{2^2}-\frac{1}{3^2}\Big)\Big(1-\frac{1}{2^{1/2}}\Big).$$

The next stepsize proposal is gained from (44) by computing τ^* as the root of a scalar function. In the case of vanishing $\bar{\mathbf{X}}(t+\tau)$, the defining equation (44) reduces to the classical stepsize formula (42).

Switch between no contact and contact. A certain difficulty in timestep selection arises if a switch between contact and no contact occurs in a timestep. In this case, the quantity $\bar{\mathbf{X}}$ is very large at the timepoint when the two bodies are in contact, but zero in the absence of contact. In order to ensure an efficient timestep selection, we need a suitable assumption on the behavior of this quantity in time.

For this aim, we divide the current timestep into phases of no contact, contact, and a switch between no contact and contact. The approximations with stepsize $\tau/2$ and $\tau/3$ give us the information in which part of the interval the switch occurs, cf. Figure 5.

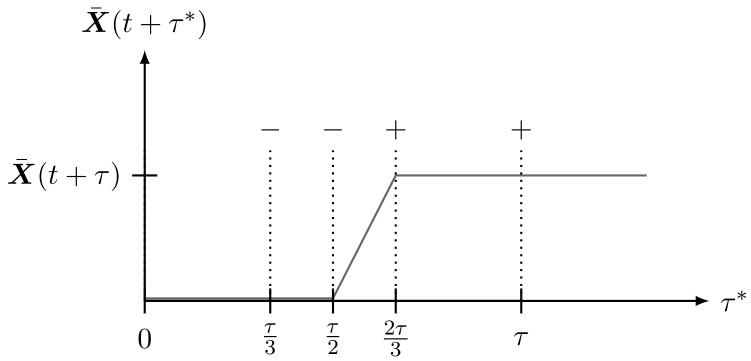

Figure 5: Model assumption on $\bar{\mathbf{X}}(t+\tau)$ ('+' and '–' indicate whether contact occurs or not).

If the stepsize τ^* touches an interval where no contact occurs, we take

$$\bar{\mathbf{X}}(t+\tau^*)=0\,,$$

and within an interval with contact, we make the assumption

$$\bar{\mathbf{X}}(t+\tau^*)=\bar{\mathbf{X}}(t+\tau)\,.$$

For a subinterval $[t_j, t_{j+1}]$ with a switch between no contact and contact, we use a linear interpolation and set

$$\bar{\mathbf{X}}(t+\tau^*) = \Big(\frac{t+\tau}{t_{j+1}-t_j} - \frac{t+t_j}{t_{j+1}-t_j}\Big) \cdot \bar{\mathbf{X}}(t+\tau)\,.$$

If we have not found contact in an accepted timestep, we access to the last rejected step with active contact boundaries. The optimal stepsize τ^* is given by (43) as the root of a scalar function.

5 Numerical illustrative example

In this section, we give an example for the adaptive timestep control ContacX of the contact–stabilized Newmark method as suggested in this paper.

The implementation of our algorithm has been done within the framework of the Distributed and Unified Numerics Environment Dune [3, 4]. For discretization in space, we have used the finite element toolbox UG [2]. The information transfer at the contact interface Γ_C is realized by means of non-conforming domain decomposition or mortar methods, see [23]. Among the possible solvers for variational inequalities, we have selected monotone multigrid methods [18, 20] since linear multigrid convergence speed can be achieved without any additional parameters. The adaptive contact solver [19] has been further improved in [10]. In practical applications, the truncated nonsmooth Newton multigrid method (TNNMG) enters the fast linear convergence almost immediately. For the $\mathbf{L}^2$-scalar product, we use a lumped mass matrix which makes the cost for computing CSN negligible.

We consider the illustrative Hertzian contact problem of Section 3.3, where we refine sixth times within the circle around the top of the semicircle. The parameters for the adaptive stepsize control are given in Table 2 where E_0 denotes the initial energy of the system.

parameter	value
tolerance TOL	$10^{-4} \cdot \mathrm{E}_0$
safety factor ρ	0.9
initial timestep	10^{-2}
maximal timestep	1
maximal growth factor for timesteps	10

Table 2: Specifications for adaptive timestep control.

Figure 6 shows the size of the adaptively chosen timesteps. When the body is entering the phase of contact, the controller reduces the timesteps significantly. The timesteps increase up to the moment when the halfcircle removes from the plate. Here, depending on the desired time tolerance, the controller may reduce the timesteps again. In the absence of contact, the timesteps grow considerably.

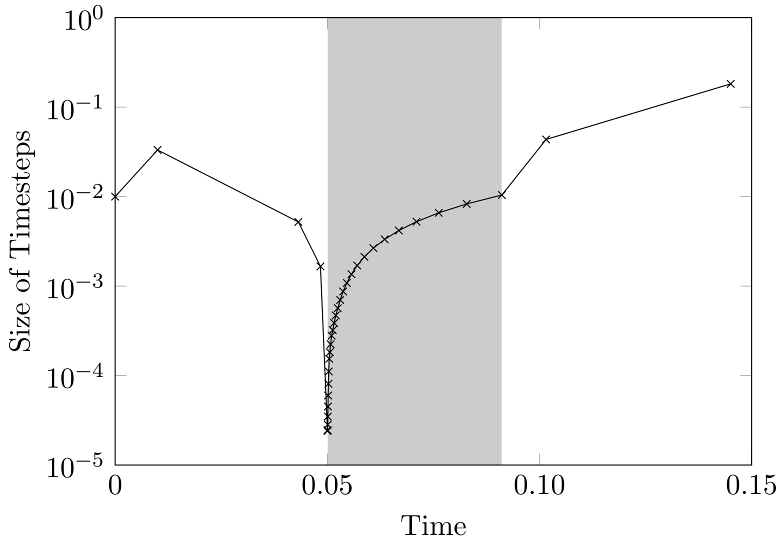

Figure 6: Timestep history beyond contact (grey: phase of contact).

For $j = 6$ and $\mathrm{TOL} = 10^{-4} \cdot \mathrm{E}_0$, the integration scheme has carried out 40 timesteps where only 4 of them have been rejected. The repeats occur when the two bodies come into contact. Table 5 contains the number of accepted and rejected timesteps for different tolerances and refinement levels of the grid. For small tolerances, the adaptive timestep control requires a sufficiently high resolution of the grid near the changing contact boundaries in order to avoid effects of spatial discretization.

j / TOL	$10^{-3} \cdot \mathrm{E}_0$	$10^{-4} \cdot \mathrm{E}_0$	$10^{-5} \cdot \mathrm{E}_0$
5	8 (2)	31 (5)	75 (15)
6	8 (2)	40 (4)	89 (13)
7	12 (3)	37 (4)	104 (11)
8	10 (2)	33 (4)	146 (9)
9	10 (2)	55 (5)	180 (10)

Table 3: Total number of timesteps (number of rejected timesteps) depending on tolerance TOL and refinement level j of the grid.

Figure 7 shows the time evolution of the physical energy norm of $\bar{\mathbf{X}}$. The norm becomes extremely large at the timepoint when the two bodies come into contact. In Figure 8, we see the spatial distribution of $\dot{\mathbf{X}}$ for a fixed time. As expected, the quantity is located near the part of the possible contact boundaries where the active set changes.

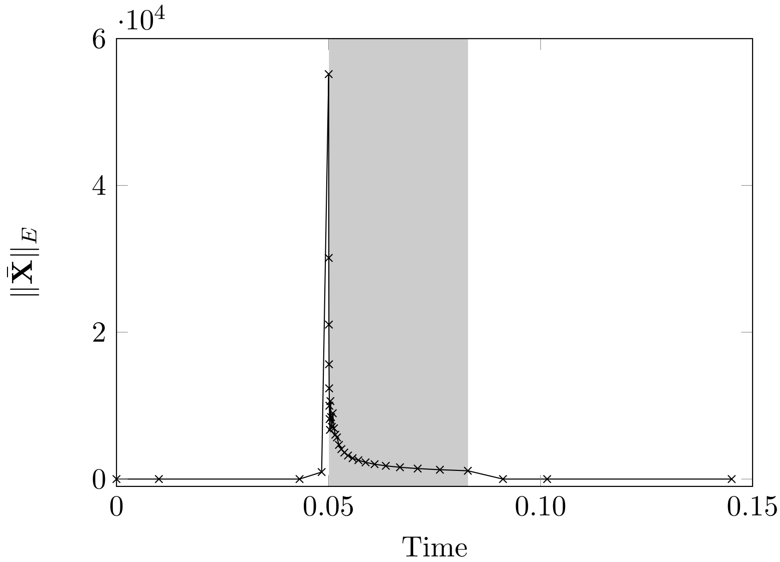

Figure 7: Time evolution of $\|\bar{\mathbf{X}}\|_E$ (grey: phase of contact).

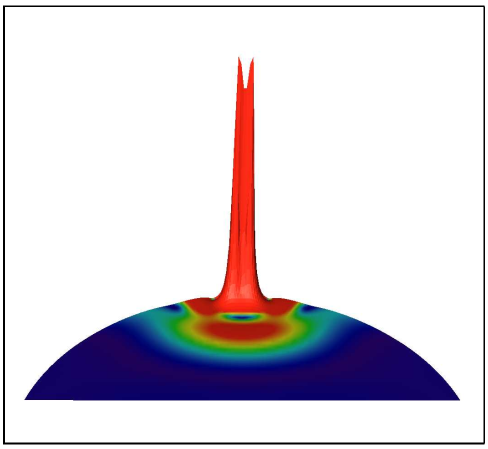

Figure 8: Estimated spatial distribution of $\dot{\mathbf{X}}(t+\tau)|_{t=0.051}$.

6 Conclusion

The paper has suggested an adaptive timestep control in the contact–stabilized Newmark method for dynamical contact problems (ContacX). Both theoretical analysis and numerical experiments have led to a perturbed asymptotic error expansion of the scheme. We have constructed an error estimator via modified extrapolation techniques and a problem-adapted timestep size selection. First numerical experiments exhibit a close connection between our new theory and our numerical findings.

Acknowledgment. The authors thank Martin Weiser, Zuse Institute Berlin, for helpful discussions on the topic of this paper and Oliver Sander, FU Berlin, for his support with the multigrid solver for the stationary contact problems.

References

[1] J. Ahn and D. E. Stewart. Dynamic frictionless contact in linear viscoelasticity. *IMA J. Numer. Anal.*, pages 1–29, 2008.

[2] P. Bastian, K. Birken, K. Johannsen, S. Lang, N. Neuß , H. Rentz–Reichert, and C. Wieners. UG – a flexible software toolbox for solving partial differential equations. *Comput. Vis. Sci.*, 1:27–40, 1997.

[3] P. Bastian, M. Blatt, A. Dedner, C. Engwer, R. Klöfkorn, R. Kornhuber, M. Ohlberger, and O. Sander. A generic interface for parallel and adaptive scientific computing. Part II: Implementation and tests in DUNE. *Computing*, 82(2–3):121–138, 2008.

[4] P. Bastian, M. Blatt, A. Dedner, C. Engwer, R. Klöfkorn, M. Ohlberger, and O. Sander. A generic interface for parallel and adaptive scientific computing. Part I: Abstract framework. *Computing*, 82(2–3):103–119, 2008.

[5] P. Deuflhard and F. Bornemann. *Scientific Computing with Ordinary Differential Equations*, volume 42 of *Texts in Applied Mathematics*. Springer, 2002.

[6] P. Deuflhard, R. Krause, and S. Ertel. A Contact-Stabilized Newmark method for dynamical contact problems. *Internat. J. Numer. Methods Engrg.*, 73(9):1274–1290, 2007.

[7] G. Duvaut and J. L. Lions. *Inequalities in Mechanics and Physics*. Springer, 1976.

[8] C. Eck. *Existenz und Regularität der Lösungen für Kontaktprobleme mit Reibung*. PhD thesis, Universität Stuttgart, 1996.

[9] I. Ekeland and R. Temam. *Convex Analysis and Variational Problems*. North–Holland, Amsterdam, 1976.

[10] C. Gräser and R. Kornhuber. Multigrid methods for obstacle problems. *J. Comp. Math.*, 27:1–44, 2009.

[11] E. Hairer and C. Lubich. Asymptotic expansions of the global error of fixed-stepsize methods. *Numer. Math.*, 45:345–360, 1982.

[12] E. Hairer, C. Lubich, and G. Wanner. *Geometric Numerical Integration. Structure–Preserving Algorithms for Ordinary Differential Equations.* Computational Mathematics. Springer, Berlin, Heidelberg, 2nd edition, 2006.

[13] C. Kane, E. A. Repetto, M. Ortiz, and J. E. Marsden. Finite element analysis of nonsmooth contact. *Comput. Methods Appl. Mech. Engrg.*, 180:1–26, 1999.

[14] N. Kikuchi and J. T. Oden. *Contact Problems in Elasticity.* SIAM, Philadelphia, 1988.

[15] C. Klapproth. *Adaptive numerical integration for dynamical contact problems.* PhD thesis. In preparation.

[16] C. Klapproth, P. Deuflhard, and A. Schiela. A perturbation result for dynamical contact problems. *Numer. Math. Theor. Meth. Appl.*, 2(3):237–257, 2009.

[17] C. Klapproth, A. Schiela, and P. Deuflhard. Consistency results on Newmark methods for dynamical contact problems. *Numer. Math.*, published online, 26 March 2010. `http://www.springerlink.com/content/72jq2430122253v2/`.

[18] R. Kornhuber and R. Krause. Adaptive multilevel methods for Signorini's problem in linear elasticity. *Comput. Vis. Sci.*, 4:9–20, 2001.

[19] R. Kornhuber, R. Krause, O. Sander, P. Deuflhard, and S. Ertel. A Monotone Multigrid Solver for Two Body Contact Problems in Biomechanics. *Comput. Vis. Sci.*, 11(1):3–15, 2008.

[20] R. Krause. *Monotone Multigrid Methods for Signorini's Problem with Friction.* PhD thesis, FU Berlin, 2000. `http://www.diss.fu-berlin.de/diss/receive/FUDISS_thesis_000000000469`.

[21] F. Mignot. Contrôle dans les inequations variationelles elliptiques. *J. Funct. Anal.*, 22:130–185, 1976.

[22] E. Schechter. *Handbook of Analysis and Its Foundations.* Academic Press, 1997.

[23] B. Wohlmuth and R. Krause. Monotone methods on nonmatching grids for nonlinear contact problems. *SIAM J. Sci. Comput.*, 25(1):324–347, 2003.

[24] E. Zeidler. *Nonlinear Functional Analysis and Applications II A/B.* Springer Verlag, 1990.